Flash flooding hazard assessment, modeling, and management in the coastal zone of Ras Ghareb City, Gulf of Suez, Egypt

Mohamed O. Arnous[1] · Ahmed E. El-Rayes[1] · Habash El-Nady[2] · Ahmed M. Helmy[2]

Abstract

The assessment of flash flood hazards in the coastal zone of Ras Ghareb City (RGC), Red Sea, Egypt, was accomplished through the use of GIS tools and the spatial multi-criteria approach. The presented work aims to assess, integrate, and generate potential flash flood hazard maps. The analytic hierarchy process was utilized to calculate weights of hazard and vulnerability of flash flood controlling factors and their parameters such as topographical, geological, and hydrological factors. In addition, the risk degree of each specific basin and its sub-basins is estimated by combining standardized parameter values. Despite its location in an arid region, the basin may receive a large amount of rainwater, which can cause flash floods at the basin's outlet. Recently, flash flooding took place in the coastal region of RGC in October 2016 and September 2020, resulting in the loss of many human lives and catastrophic effects on local infrastructure and surrounding environments. According to reports from Hurghada, Red Sea Governorate, the RGC experienced exceptional flooding that exceeded 120 million cubic meters as a result of 51 mm of rainfall. Based on the remote sensing satellite data such as Aster Digital Elevation Model (GDEM) and the GIS tools, the basin and sub-basin drainage patterns were delineated and compared with reference topographical map sheets of a scale of 1: 50,000. The sub-basins have been isolated and morphometrically studied to determine vulnerability to flash flooding. In addition, the flash flood threat model was developed using geoprocessing tools provided by ArcGIS software to incorporate all contributing factors spatially. The flash flood risk in the Ras Ghareb (RG) basins and their sub-basins has been identified and classified into three classes (high, medium, and low hazard degree). High and moderate flood-risk basins require comprehensive studies to introduce measures to protect certain areas from flood danger. Finally, the GIS and the spatial multi-criteria analyses were effective ways to carry out a flash flood management system in order to support the decision-makers by recommendations to conserve and mitigate the possible flash flood hazards in the study areas.

Keywords Flash flood · Ras Ghareb · GIS · Remote sensing · Hazard · Morphometric parameters

Introduction

Coastal areas are home to significant natural and economic resources, but in many parts of the world, these resources are either underutilized or utilized in ways that do not completely optimize sustainable development. For instance, several countries have developed the lowlands around their coasts into places for farming, habitation, domestic timber, and food production. People have a long-standing romantic bond with coastal regions going back to the dawn of civilization. Coastal cities are experiencing an increase in the frequency, severity, and effects of coastal flooding. The severity of floods is influenced by a variety of factors, including urban growth, expanded building, the installation of other assets near the shore, and climate change (Hallegatte et al. 2013; Arnous and Omar 2018; Dhiman et al. 2019; Dube et al. 2022). Furthermore, several factors, particularly uncontrolled urban growth, climate change, and sea level rise, contribute to the hydrological hazards that coastal communities must manage. Extreme weather events and flash flooding have accelerated as a consequence of climate change, posing new challenges for economic growth and the environment of coastal communities. Flash floods are among

✉ Mohamed O. Arnous
  mohamed.arnous@science.suez.edu.eg;
  arnous_72@yahoo.com

1 Geology Department, Faculty of Science, Suez Canal University, Ismailia, Egypt

2 Geology Department, Faculty of Science, Arish University, Arish, Egypt

the world's catastrophic natural hazards which cause the greatest number of deaths and property damage (CEOS 2003; El-Rayes et al. 2009; Arnous et al. 2011; Arnous and Green 2011; Arnous and Omar 2018; Moubarak et al. 2021; Omran et al. 2021). Floods, because of their disruptive nature, can have an impact on many aspects of human existence and can result in significant costs for mitigation measures. Smith (2013) suggested that flooding annually takes more than 20,000 lives each year and damages about 75 million people worldwide. The majority of floods are caused by frontal or convective storms paired with intense, protracted rain. Additional interrelated factors that affect the intensity of flash floods include rainfall characteristics, water loss (via evaporation and infiltration), drainage networks, drainage ordering, drainage characteristics, and environmental and human activities (Saleh 1989). Topography, geomorphology, drainage, infrastructure systems, and climate are key factors leading to flooding problems (Youssef et al. 2011; Arnous 2011). Furthermore, the topographical and geomorphological features, details such as the existence of the boundaries of the wadis and their network drainage systems. The characteristics of the drainage network basin in various dry zones throughout the world were investigated using the principles of geomorphological methodologies, which are primarily based on Horton (1945) and Strahler (1964). The morphometric characteristics of the analysis of the network basins derived from digital remote sensing (RS) data were used to estimate, define, evaluate, forecast, and define the relationships between the morphometric characteristics of the basin and the potential for flash flood risk and its environmental impacts (Patton 1988; Gardiner 1990; Sameena et al. 2009; Nageswararao et al. 2010; Arnous et al. 2011; Arnous and Omar 2018). Characterization of drainage plays a major role in determining flash flood danger (Dawod et al. 2012). Geomorphology has been widely important to fluvial systems (Thorne 2002), thus worldwide studies have defined drainage networks based on conventional geomorphological methods in basins and sub-basins (Horton 1945; Strahler 1964; Krishnamurthy et al. 1996). Quantitative measurements of drainage basins and their geometrical properties are widely used in watershed research (Abrahams 1984). Therefore, each basin's morphometric variables may properly reflect the distribution of runoff, the peak of floods, the estimates of erosion, the yields of sediment, and the implications of floods (Patton 1988; Gardiner 1990). In this study, watershed terrain analysis was employed to categorize the morphometric parameters of the catchments in the RG region and their drainage network. Its procedure also included identifying the major rock unit types and conducting an in-depth investigation of the various geological features. Any arid mountainous area can benefit from the integration process, which employs

RS and Geographic Information Systems (GIS) tools to detect and quantify flash flood hazards. In addition to GIS, data from space-borne RS suggest promising alternatives to predictable approaches for assessing, integrating, and mapping various types of natural hazard events. Numerous studies have been published all over the world to demonstrate how RS and GIS approaches can be employed to explore, map, and reduce potential threats in flash floods, especially in arid regions (Zerger and Smith 2003; Bapalu and Sinha 2005; Fernandez and Lutz 2010; Arnous et al. 2011; Arnous and Green 2011; Youssef et al. 2011; Bajabaa et al. 2014; El-Rayes and Arnous 2015; El-Rayes et al. 2015, 2017; Arnous et al. 2020; Arnous and Mansour 2022). The GIS is a basic technology for evaluating, controlling, and integrating the factors that lead to flash flood threats with high precision and efficiency (Abuzied et al. 2016). In this investigation, the GIS was used to build and incorporate the causes of flash floods into a single georeferencing framework. When mapping the flash flood hazard, ratings for each factor's relevance, as well as weights for its classes based on flash flood hazard contributions, are required (Dawod et al. 2012). Therefore, in this study, the statistical analysis of the commutative weights was used to assign appropriate ranks for contributing factors to the flash flood. The goal of our research is to look into a new flash flood threat model that incorporates multi-factor analysis. These factors include lithology, slope, hydrological morphometries, elevation, structure lineament density, runoff, and rainfall volume. The integrated methodology results in a more precise flash flood threat map, which is an important tool for mountainous development planning.

The study area, the Eastern Desert of Egypt, is well known for being a flood-prone area where flash flooding is frequently documented, resulting in significant infrastructure damage, community displacement, and occasionally fatalities. It is characterized by its rugged terrain and steep mountains. Several authors have studied the geomorphology and geology of the region, including Ball (1916); Shata (1955); Hammad (1980); Saad et al. (1980); El Shamy (1983); Hammad and Misak (1985); Aglan (1995); Aggour and Gomaa (2008). In addition, the area's precipitation occurs with long dry summers during the fall, winter, and spring. For several successive years, the region may be subject to a separate dry climate. Intense rainstorms with short moments may occur once every three to four years, resulting in catastrophic floods (El Shamy 1983).

The current work is an attempt to analyze, assess, model, and manage the flash flood hazards potentiality of the study area using the RS and GIS tools. To accomplish these attempts, the identification of the climatic conditions that controlled the area and the adjacent region was required. Recognition will be explored regarding the effect of topography, lithology, and geological structures on the basin system.

Furthermore, in view of the surface runoff ability, the development of the drainage network and determination of the morphometric parameters of the hydrographic basins and their hydrological importance will be achieved.

Study area

The RGC area is located west of the Gulf of Suez between longitudes 32° 10′ and 33° 10′ E and latitudes 28° 00′ and 28° 30′ N, and it encompasses approximately 4047 km² (Fig. 1). The RG area is covered by Precambrian igneous and metamorphic basement rocks that are exposed mainly at the central parts of the area. The Paleozoic rocks and Quaternary sediments are mostly exposed in the east and west sides (Stern and Hedge 1985).

The geography of the RG basins gradually shifts from rugged mountains to gently rolling plains that slope into the Gulf of Suez. The terrain in the research area ranges from low zones to high, steep mountains with elevations ranging from 0 to 1,687 m (Fig. 2). Several wadis (valleys) represent distinct drainage systems that cross the study area. During quaternary times and rainy periods, different cycles of sedimentation formed the wadis (Youssef and Hegab 2005).

Based on records of two meteorological stations located at Suez and Hurghada, the climate regime in the RG region is confirmed. The measurements of the meteorological elements were obtained from the Climatic Atlas of Egypt (2006) in the present research. The Red Sea Government is part of a region that falls within the arid belt. It has low precipitation, high evaporation and hot long summer temperatures, and cool short winters. Every few years, the RG region experiences heavy rainstorms sometimes causing devastating floods that run off into the Suez Gulf. Floods and groundwater recharge are influenced by climate parameters (temperature, relative humidity, surface wind, and rainfall), which also shape the various geomorphic units of the region. The lowest and highest recorded temperatures in the study region at the Hurghada meteorological station are 15.90 °C and 30.31 °C, respectively. The lowest and highest monthly evaporation values are 10 mm/day and 19.4 mm/day, respectively, while the average yearly mean is 14.3 mm/day. The annual relative humidity ranges from 49.1% to 54.6%. The RG region experiences very little, inconsistent, and limited precipitation. Every year, there is an average of 2.1 mm of precipitation in January, and 2.8 mm in December. The most rain ever recorded fell on November 16, 1996, totaling 110.4 mm (Egyptian Meteorological Authority 2006). Flash flooding occurred recently in the RG coastal region in October 2016 and September 2020, resulting in the loss of many human lives and catastrophic effects on local infrastructure and surrounding environments. Hurghada, Red Sea Governorate, experienced historic flooding that exceeded 120 million cubic meters as a result of 51 mm of rainfall, according to reports.

Materials and methods

The available data was used to determine the flash flood hazards as RS data in three formats. It is defined by the "Landsat 7 Enhanced Thematic Mapper" (ETM7+) and "Landsat 8 Operational Land Imager" (OLI) dated 2000 and 2016 respectively. Two available images cover the study area
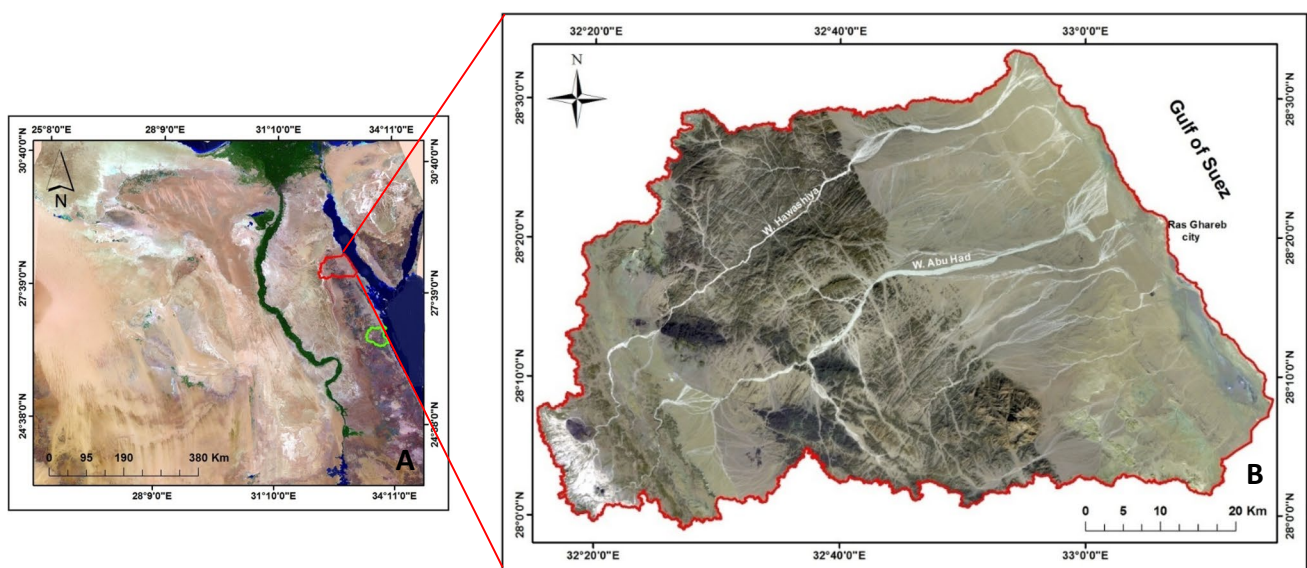

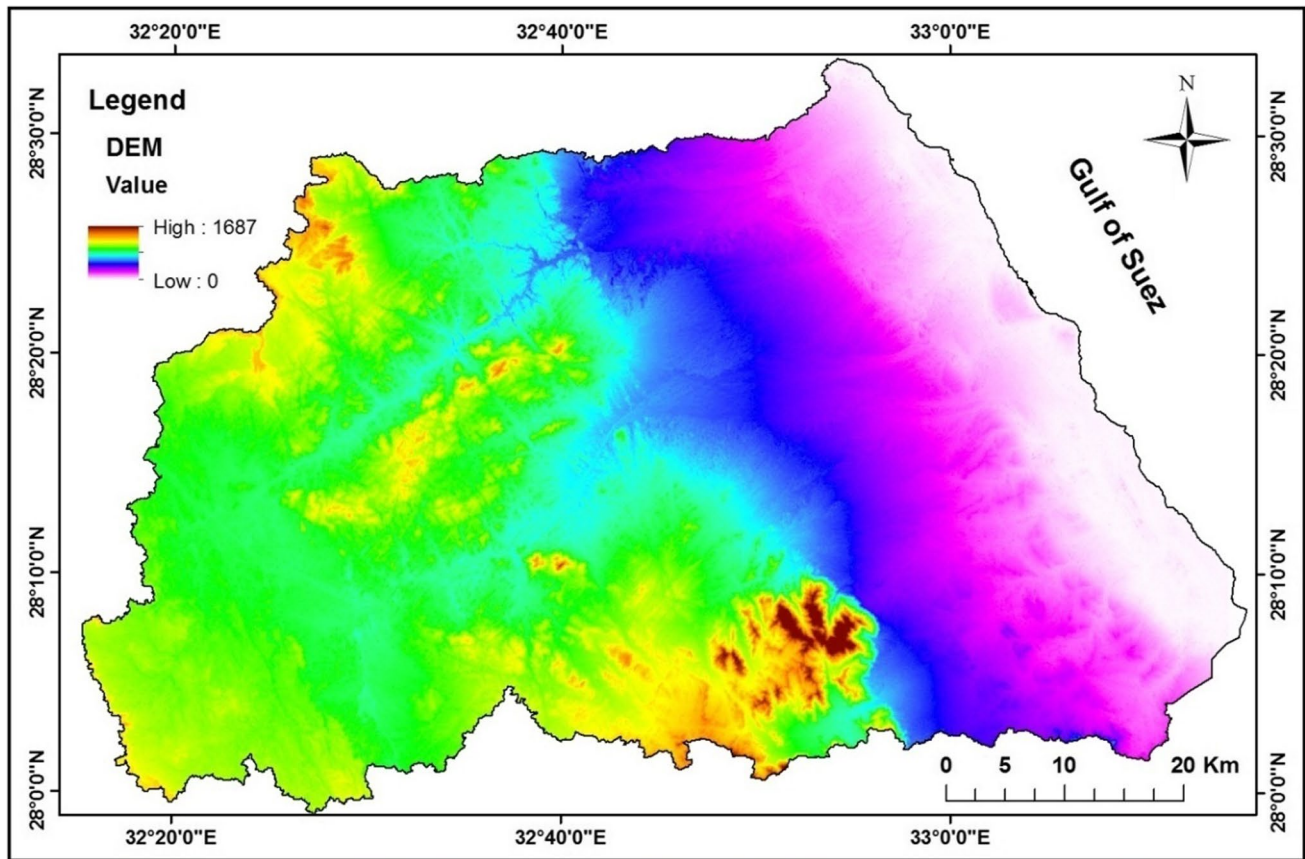**Fig. 1** Location map (**A**) and satellite image (**B**) of RG study area (Source: https://earthexplorer.usgs.gov/)

Fig. 2 Aster GDEM satellite data of RG study area (Source: https://earthexplorer.usgs.gov/)

for Path 175/ Row 40 and Path 175/ Row 41 with ground resolution (15*15 m) after merge resolution. In addition, "Advanced Spaceborne Thermal Emission and Reflection" (ASTER) data dated, 2009 two scenes covering the study area with 30 * 30 m grid cell size. ASTER GDEM data is used to conduct field analysis and to detect the geological, topographical, and geomorphological characteristics of the terrain. In order to determine catchments affecting infrastructure efficiency in the RG area, specifically in the eight network basins (Wadi (W.) Hawashiya, W. Hawashiya 2, W. Bakr 1, W. Bakr 2, W. Bakr 3, W. Abu Had, W. Gharib, and W. Garf), terrain analyses of the RG area's landforms, elevations, slope, aspect, and curvature were performed using the GDEM (Fig. 3). Using the WGS 84 datum, these RS data are corrected into a zone 36 North Universal Transverse Mercator (UTM) projection. During the pre-processing phase of obtained datasets, image rectification, pixel resampling, radiometric, and atmospheric (FLAASH) corrections are all performed. Geo-reference data is provided by maps of various types and scales covering the research area. Additional tabular and auxiliary data, such as 1:50,000 scale topographic and geological maps, also are readily accessible and used. Many descriptive datasets, such as meteorological data,

are collected and incorporated as GIS layers. The results of lithological, structural, geomorphological, and morphometric analyses were acquired and extracted using ERDAS Imagine 14, ArcGIS 10.3, and STATISTICA 7. Band ratios, end member selection, minimal noise fraction (MNF), principle component analysis (PCA), and terrain analysis are the seven techniques that are primarily used to eliminate different types of class borders, including slope, aspect, curvature, and hill-shade. GIS tools have been developed to be useful in delineating and extracting stream networks from DEM data; in assessing and managing flash flood risk management (Maidment 2002; Zhang et al. 2009; Omran et al. 2011; Arnous 2016; Arnous and Omar 2018) (Fig. 4). Morphometric parameters of the RG network basins were primarily based on the use of Arc Hydro instruments in the ArcGIS spatial analyst extracted and mapped to the watershed area. The watershed characteristics and morphometric parameters were automatically extracted based on Arc Hydro operational processes such as fill sinks, flow direction, stream definition, stream segmentation, and stream order (Kumar et al. 2000; Zhang et al. 2009; Omran et al. 2011; Rai et al. 2014; Arnous 2016; Arnous and Omar 2018).
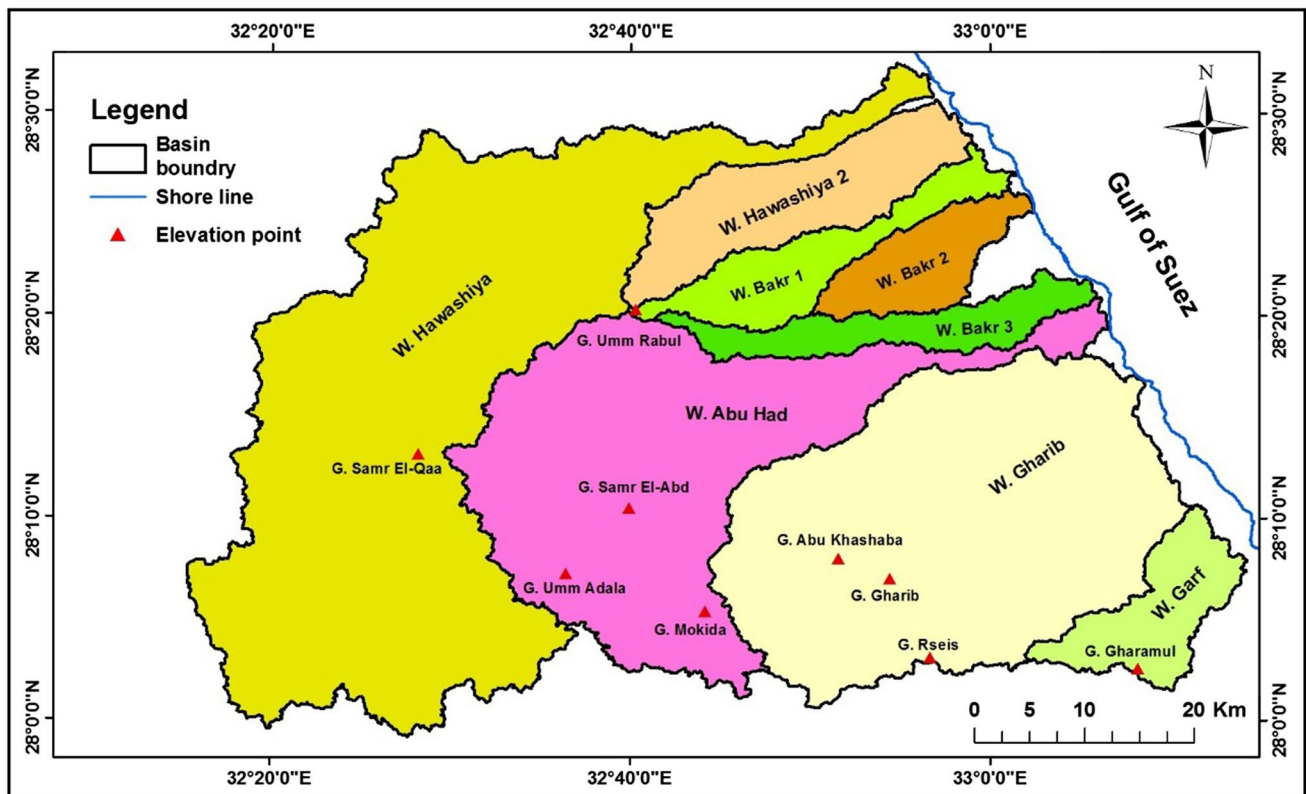
Fig. 3 Main hydrographic basins of RG area

Filling sinks were used to check proper basin and stream network delineation. The filling attaches pixels displaying downslope flow in the surrounding areas. The direction of flow is determined by the steepest path falling from each cell, this step continued after the depressions were associated. This showed the path of downslope flowing out of every cell. The output of the flow accumulation would show the amount of rainfall that would flow through each pixel of the cell. This proves that all of the precipitation that accumulated was converted to runoff without any interception, evaporation, or infiltration (Xiao et al. 2010). This could also be seen as the sum of rain falling from each cell to the surface, upslope. Thus, the accumulation of flow can be used to obtain a stream network by applying a threshold value to select highly accumulated cells (El Nahry and Saleh 2005; Wang et al. 2010). The stream network is drawn from GDEM to develop and build the RG stream network and order maps. Stream order is the mean by which the stream basin network transmits a numerical order to the relatives. In the current study, the Strahler approach is used to categorize mega-basin systems that are assigned to the W. Hawashiya, W. Abu Had, and W. Gharib mega basins in the sixth order. During the delineation of drainage basins, watershed techniques are used to define the water divide between sub-basins in order to ensure the selection of areas with significant accumulated

runoff (Omran et al. 2011). The results of this approach established and defined the sub-basins comprised in each of the three mega basins in the RG area, which were then categorized, mostly based on their watershed size, total length, and the number of segments. The morphometric parameters are used to determine the potential for severe flooding. Therefore, the morphometric parameters of drainage basins and their network channel are listed in the Table 1 along with their mathematical formula. These parameters can be divided into four main groups: drainage network parameters, basins geometry parameters, drainage texture parameters, and basin relief parameters (Martz and Garbrechet 1992; Kumar et al. 2000; Arnous et al. 2011; Omran et al. 2011; Mondal and Gupta 2015). Finally, GIS is used to incorporate statistical analysis of the commutative weights of the derived basin morphometric parameter data. The potential flash flood hazard areas were compared and ordered using the risk-level categories of high, moderate, and low. It was possible to distinguish between the lithological and geomorphological units of the investigated region by using a variety of spectrometric mapping techniques, including histogram equalization, best band combination, band ratio, like-hood classification, spatial filtering, and PCA techniques on the enhanced OLI, ETM7 +, and ASTER imageries. Using GIS and digital image processing tools, the surface analysis
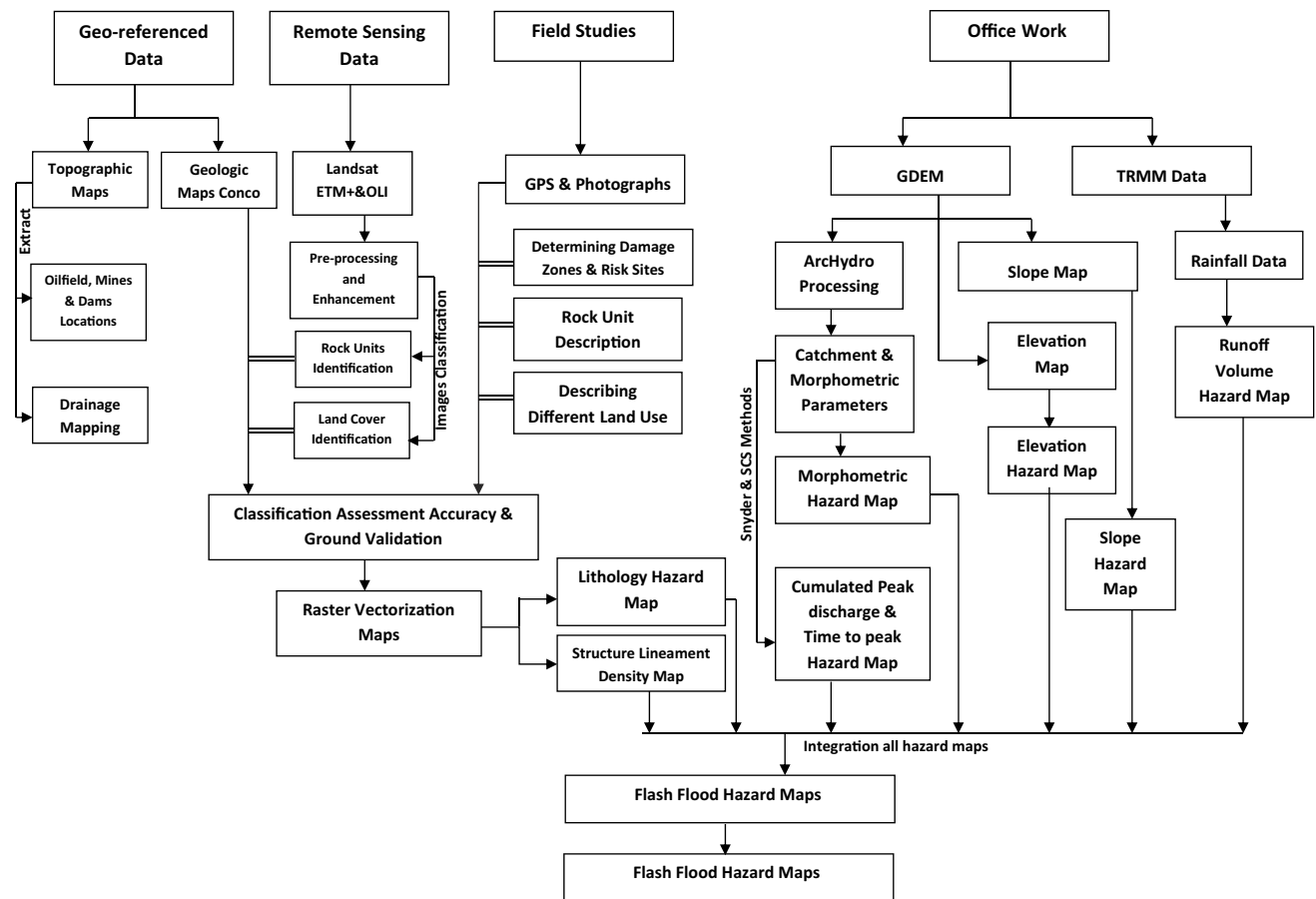
Fig. 4 Flow chart shows all data and methods that were used to assess flash flood hazards

of the RG region, including slope, aspect, curvature, and hill shading, is extracted from the digital elevation model (GDEM).

Preparation of the geo-spatial thematic modeling and flash flood hazard potentiality maps

RS and GIS data are incorporated into the present study to delineate the area most vulnerable to flooding in the RG area. Geospatial tools were effectively used to classify and delineate areas, as well as to create spatial distribution maps of flood accumulation possibilities based on various factors. In order to build a flash flood potential map, a linear combination of these variables was combined using an ArcGIS spatial analytic mode. Some of the various thematic geospatial maps mentioned in the preceding have been converted into raster form. These were then reclassified, and sufficient weights were allocated. The selected factors assessed were used to estimate the study area's flash flood risk levels. Seven variables are viewed as layers inserted into a model. All these variables are believed to be addressed in the entire field of study and are of equal importance. These factors are:

(1) Morphometric parameters, the evaluation of each morphometric parameter is based on the causative relationship between its values and the intensity of a flash flood. Based on its characteristics and relevance to the degree of flooding, each parameter is classified into one of three classes.

(2) Cumulated runoff, extreme flash floods caused by violent storm events cause extensive destruction, fatalities, and property damage. It is feasible to understand these flash floods, despite the fact that they are a complex natural phenomenon, by examining how the interaction of topographical features and meteorological extremes contributes to favorable flooding conditions.

(3) Lithological units, they are an important indicator for determining flash flood risk areas. The majority of the Precambrian basement rocks in the study area have been subjected to extensive mechanical weathering, making them brittle and prone to disintegration. The worn, disintegrating rocks along structural lineaments and cracks cause an excessive amount of water to flow down drainage channels, specifically on steep slopes and after intense rainfall.

Table 1 Morphometric parameters and their mathematical formula

Morphometric Parameters			Formula	Reference
Drainage Network	1	Stream order (u)	Hierarchical rank	Horton (1945), Strahler (1952, 1964)
	2	Stream number (N_u)	$N_u = N1 + N2 + \cdots + N_n$	Strahler (1952)
	3	Stream length (L_u) km	$L_u = L1 + L2 + \cdots + L_n$ (km)	Strahler (1964), Horton (1932)
	4	Mean stream length (L_{sm}) km	$L_{sm} = L_u/N_u$ (km)	Strahler (1964)
	5	Stream length ratio (R_L)	$R_L = L_u/L_u - 1$, where L_u = the total stream length of order, $L_u - 1$ = the total stream length of its next lower order	Horton (1945)
	6	Bifurcation ratio (R_b)	$R_b = N_u/N_u + 1$, where N_u = total no. of stream segments of order, $N_u + 1$ = no. of segments of the next higher order	Schumn (1956)
	7	Mean bifurcation ratio (R_{bm})	R_{bm} = average of bifurcation ratio of Strahler all orders	Strahler (1957)
Basin Geometry	8	Basin length (L_b) km	GIS software Analysis	Schumn (1956)
	9	Basin area (A) km^2	GIS software Analysis	Schumn (1956)
	10	Basin perimeter (P) km	GIS software Analysis	Schumn (1956)
	11	Form factor (ratio) (R_f)	$R_f = A/L_b^2$	Horton (1945)
	12	Circularity ratio (R_c)	$R_c = 4\pi A/P^2$	Strahler (1964), Miller (1953)
	13	Elongation ratio (R_e)	$R_e = 1.128 \sqrt{A}/L_b$	Schumn (1956)
	14	Shape factor (B_s)	$B_s = L_b^2/A$	Horton (1945)
	15	Lemniscate ratio (k)	$K = L_b^2/4A$	Chorely et al. (1957), Ivanova et al. (2012)
	16	Drainage texture (D_t)	$D_t = N_u/P$, where N_u = Total no. Streams of all orders, P = perimeter	Horton (1945)
	17	Basin width (B_w) Km	$B_w = A/L_b$ (km)	Horton (1932)
Drainage Texture	18	Stream frequency (F)	$F = N_u/A$	Horton (1945)
	19	Drainage density (D) km/km^2	$D = L_u/A$	Horton (1945)
	20	Drainage intensity (D_i)	$D_i = F/D$	Faniran (1968)
	21	Length of overland flow (L_o) km	$L_o = 1/2D$	Horton (1945)
	22	Infiltration number (F_n)	$F_n = (F)(D)$	Faniran (1968)
Relief Characteristics	23	Maximum elevation (H_{max})	GIS software Analysis using DEM	
	24	Minimum elevation (H_{min})	GIS software Analysis using DEM	
	25	Basin relief (H)	$H = H_{Max} - H_{min}$	Hadley and Schumn (1961), Strahler (1952)
	26	Relief ratio (R_r)	$R_r = H/L_b$	Strahler (1964)
	27	Ruggedness number (R_n)	$R_n = D*(H/1000)$	Strahler (1964)

(4) Slope degree, when evaluating the likelihood of existing flash flood dangers, slope degree is among the most crucial factors. The slope, which determines how steep or inclined a surface is and influences how quickly water flows, is one of the most important factors influencing floods.

(5) Elevation, for a comprehensive assessment of the flash flood threat, elevation is a crucial factor since it influences runoff flow direction and velocity, flood extents, and depths.

(6) Structural lineaments, different levels of stress cause rock fracturing, which is represented by structural lineaments of varying densities and produces some weakness zones in weathered rocks. In terms of capacity for runoff infiltration and relevance to flooding potentiality, the weakness zones with varying lineament densities were ranked as high, moderate, and low.

(7) Runoff volume and rainfall intensity, intense rainfall and a significant amount of runoff are the primary causes of the severe flash flood in the study region. Intense rain along the upstream catchments causes enormous runoff quantities, which commonly flow into the down streams. Predicting the likelihood of flash floods requires knowledge of runoff volume.

Integrating the aforementioned data may reveal high flash flood risk areas in the research area. The quantitative values associated with all types of data should be assigned a distinct score on a scale based on how serious a flood or risk is. Then, an overlay activity will compare the intersected locations based on the sum of the scores, assigning a score to each region based on its risk of flooding. Each factor is assessed using a simple statistical technique based on the correlation between the values of the factors and the potential of flash floods (Pradhan 2010; Youssef et al. 2011). In accordance with the probable level of risk associated with each factor, everyone is divided into three categories. The variables are classified into three intervals using the formula (Max–Min)/3. Different scores on a scale are given to achieve a final assessment of flood risks according to their relevance to flood risk. An overlay procedure would analyze the intersected regions by summing up scores in order to classify each region by a score measure. The result is divided into three groups using equal intervals to provide a clear final map (low, medium, and high risk). The severity of the hazards is assigned a rating from 1 to 3. The raw score for each function is normalized using the equation below, taking into account the different parameter signs. The following equation, based on various influencing factors, estimates the flooding risk level in the study area:

$$
\begin{aligned}
\text{Integrated Flooding Risk} = \ & \text{Raw Score Morphometric parameters} \\
& + \text{Raw Score Cumulated runoff} \\
& + \text{Raw Score Lithological units} \\
& + \text{Raw Score Slope degree} + \text{Raw Score Elevation} \\
& + \text{Raw Score Lineaments density} \\
& + \text{Raw Score Runoff volume.}
\end{aligned}
$$

Results and discussion

The integrated satellite RS results and GIS data are used to determine and monitor the potential for flash flood hazards.

Morphometric parameters potentiality mapping

RG area is divided into distinguished eight mega basins; namely Wadi (W.) Hawashiya, W. Hawashiya 2, W. Bakr 1, W. Bakr 2, W. Bakr 3, W Abu Had, W. Gharib and W. Garf (Fig. 5). W. Hawashiya is subdivided into six relatively sub-basins; namely H1, H2, H3, H4, H5, and H6. W.Abu Had is sub-divided into eleven relatively sub-basins; namely AH1, AH2, AH3, AH4, AH5, AH6, AH7, AH8, AH9, AH10 and AH11. W. Gharib is subdivided into seven relatively
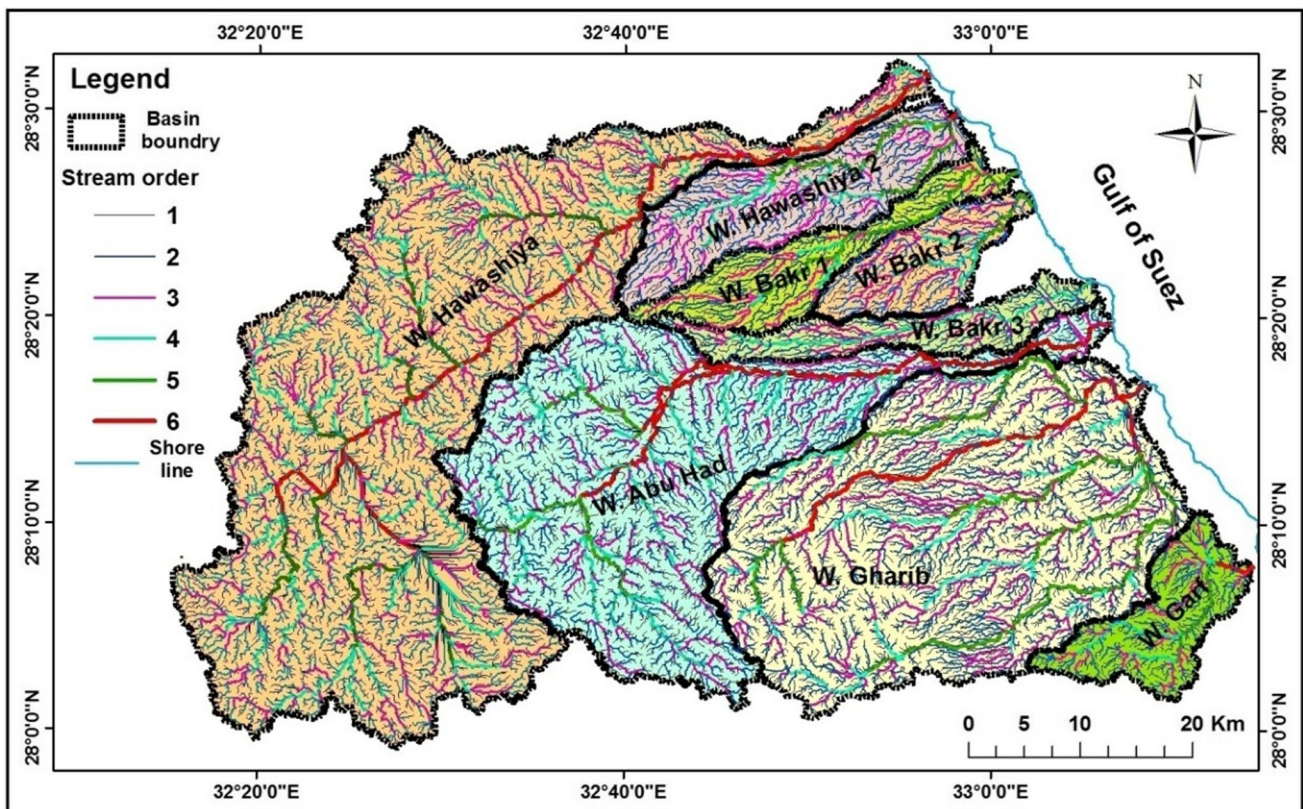

Fig. 5 Surface drainage network of RG Basins

sub-basins; namely Gh1, Gh2, Gh3, Gh4, Gh5, Gh6, and Gh7.

Internal and external drainage networks of the eight main basins are well-defined and strongly integrated. Using the ArcGIS software, the drainage maps for the basin catchment regions are obtained by extracting the drainage networks from the GDEM of the ASTER satellite image. The maps created for this technique include boundaries of the basin and maps of the drainage network. The RG hydrographic basins usually run-in directions W to E. Both wadis' main trunks open up into the coastal plain to enter the Suez Gulf (Fig. 5). The drainage network map of the RG region basins shows ranging from 4th order to 6th order according to Strahler's classification (Table 2). There is a five-stream

carrying the sixth order, while there are only two streams carrying the fifth. Tables 3 and 4 show all the morphometric parameters of RG area basins and their related sub-basin watersheds.

Using the assessed influencing factors, the research region's sub-flash basin's flood risk levels are estimated. The research area's drainage system and watershed are analyzed in light of 24 influencing factors and included as layers to the model. The importance of each of these properties is equal and they are all included throughout the entire area of research. A generic flood risk model has been developed based on causative factors such as the drainage network, basin shape, drainage texture, and terrain features. Using this model may reveal high-risk zones in the research area.

Table 2 Total number of streams (Nu) and total stream length (Lu) in Km for each stream order of the drainage basins and related sub-basins in RG area

Basin name and related sub-basins codes	1st Order N_u	L_u Km	2nd Order N_u	L_u Km	3rd Order N_u	L_u Km	4th Order N_u	L_u Km	5th Order N_u	L_u Km	6th Order N_u	L_u Km
Hawashiya (H)	4277	1848.9	938	9531.1	216	483.2	53	233.7	9	87.2	1	105.1
(H1)	1189	528.3	261	280.2	60	131.1	16	83.2	2	27.8	1	11.9
(H2)	795	327.01	181	172.5	40	86.2	11	47.3	3	19.8	1	12.9
(H3)	324	143.6	71	66.1	17	34.4	4	29.3	1	5.6		
(H4)	249	102.6	59	45.2	15	22.4	4	12.5	1	13.7		
(H5)	402	179.1	90	96.5	22	56.9	4	16.6	1	14.6		
(H6)	152	64.9	34	31.1	8	16.8	2	8.8	1	5.2		
Hawashiya 2	660	325.7	143	182.5	35	92.3	8	37.7	2	36.7	1	1.2
Bakr 1	396	187.3	74	146.1	18	58.1	4	12.1	1	34.4		
Bakr 2	318	163.3	69	94.6	13	58.01	3	22.3	1	10.5		
Bakr 3	348	189.6	72	90.1	18	63.4	1	40.6				
Abu Had(AH)	2472	1025.9	524	560.2	119	318.7	26	137.4	4	39.6	1	80.6
(AH1)	539	219.5	115	105.8	23	61.9	7	35.8	1	13.5		
(AH2)	356	140.4	80	86.7	17	31.8	5	20.5	1	12.1		
(AH3)	170	67.6	37	26.7	9	25.3	1	11.8				
(AH4)	77	31.4	17	16.8	4	11.7	1	4.4				
(AH5)	46	19.1	13	12.1	4	6.5	2	2.3	1	0.9		
(AH6)	293	109.7	71	50.2	17	35.4	4	13.8	1	12.8		
(AH7)	99	36.3	24	19.3	6	9.9	1	9.9				
(AH8)	87	38.8	19	18.2	4	9.3	1	11.1				
(AH9)	53	21.1	11	12.7	3	11.6	1	3.1				
(AH10)	39	17.9	9	7.4	2	5.9	1	6.4				
(AH11)	48	24.4	9	21.9	3	7.1	1	8.2				
Gharib(Gh)	2871	1287.9	620	693.1	128	372.7	28	127.7	6	142.5	1	54.1
(Gh1)	526	242.1	109	130.9	24	92.3	6	30.2	1	24.7		
(Gh2)	435	198.1	92	99.1	19	68.5	4	22.8	1	18.2		
(Gh3)	712	321.6	147	178.8	31	77.6	7	28	1	49.2		
(Gh4)	460	217.6	98	103.9	20	71.1	3	19.9	1	32.7		
(Gh5)	199	74.1	54	42.3	12	22.4	3	10.4	1	9.3		
(Gh6)	58	32.1	11	18.6	3	8.1	1	7.1				
(Gh7)	104	40.4	24	17.9	5	9.6	2	1.3	1	7.8		
Garf	428	209.7	98	95.6	21	49.4	5	21.3	2	12.7	1	4.1

A: Basin area; P: Basin perimeter; L_u: Stream length; N_u: Number of stream segments

Table 3 Drainage network and basin geometry morphometric parameters of basins and related sub-basins in RG area

Basin name and related sub-basins codes	Drainage Network							Basin Geometry									
	U	N_u	L_u km	L_{sm} km	R_l	R_b	R_{bm}	L_b km	A km^2	P km	R_f	R_c	R_e	B_s	K	D_t	B_w km
Hawashiya(H)	6	5494	12,289	2.236	1.45	5.57	4.73	121.2	1372	344	0.093	0.14	0.19	10.7	2.68	15.9	11.3
(H1)	6	1529	1062.5	0.694	0.47	4.53	3.73	47.28	374	152	0.167	0.20	0.26	5.97	1.49	10.0	7.91
(H2)	6	1031	665.71	0.645	0.52	3.84	3.05	38.28	247	123	0.168	0.20	0.26	5.93	1.48	8.38	6.45
(H3)	5	417	279	0.669	0.50	4.24	3.43	26.51	102	52	0.145	0.47	0.24	6.89	1.72	8.01	3.84
(H4)	5	328	196.4	0.598	0.64	3.97	3.17	21.05	77	59	0.173	0.27	0.26	5.75	1.43	5.55	3.65
(H5)	5	519	363.7	0.700	0.57	4.51	3.69	27.87	139	76	0.178	0.30	0.26	5.58	1.39	6.82	4.98
(H6)	5	197	126.8	0.643	0.53	3.68	2.90	18.85	49	43	0.137	0.33	0.23	7.25	1.81	4.58	2.59
Hawashiya 2	6	848	676.1	0.797	0.49	3.81	3.03	47.75	231	103	0.101	0.27	0.20	9.87	2.46	8.23	4.83
Bakr 1	5	493	438	0.888	1.05	4.49	3.67	48.68	143	107	0.060	0.15	0.15	16.5	4.14	4.60	2.93
Bakr 2	5	404	348.71	0.863	0.51	4.31	3.50	30.79	114	65	0.120	0.33	0.22	8.31	2.07	6.21	3.70
Bakr 3	4	439	383.7	0.874	0.60	8.94	8.08	48.97	126	112	0.052	0.12	0.14	19.0	4.75	3.91	2.57
AbuHad(AH)	6	3145	2162.4	0.687	0.77	4.83	4.01	89.58	798	237	0.099	0.17	0.20	10.0	2.51	13.2	8.90
(AH1)	5	685	436.5	0.637	0.50	4.99	4.16	30.9	166	88	0.173	0.26	0.26	5.75	1.43	7.78	5.37
(AH2)	5	459	291.5	0.635	0.55	4.38	3.57	19.7	111	75	0.286	0.24	0.34	3.49	0.87	6.12	5.63
(AH3)	4	217	131.4	0.605	0.60	5.90	5.06	20.9	49	58	0.112	0.18	0.21	8.91	2.22	3.74	2.34
(AH4)	4	99	64.3	0.649	0.53	4.25	3.45	10.6	25	27	0.222	0.43	0.30	4.49	1.12	3.66	2.35
(AH5)	5	66	40.9	0.619	0.47	2.69	1.97	6.5	14	18	0.331	0.54	0.36	3.01	0.75	3.66	2.15
(AH6)	5	386	221.9	0.574	0.62	4.13	3.33	21.8	89	58	0.187	0.33	0.27	5.33	1.33	6.65	4.08
(AH7)	4	130	75.4	0.58	0.68	4.70	3.88	11.7	30	32	0.219	0.36	0.29	4.56	1.14	4.06	2.56
(AH8)	4	111	77.4	0.697	0.72	4.44	3.62	19.7	29	47	0.074	0.16	0.17	13.3	3.34	2.36	1.47
(AH9)	4	68	48.5	0.713	0.59	3.82	3.04	9.2	18	24	0.212	0.39	0.29	4.70	1.17	2.83	1.95
(AH10)	4	51	37.6	0.737	0.76	3.61	2.84	13.4	14	32	0.077	0.17	0.17	12.8	3.20	1.59	1.04
(AH11)	4	61	61.6	1.009	0.79	3.77	2.99	16.1	19	34	0.073	0.20	0.17	13.6	3.41	1.79	1.18
Gharib(Gh)	6	3653	2678	0.733	0.58	4.94	4.11	62.34	927	163	0.238	0.43	0.31	4.19	1.04	22.4	14.8
(Gh1)	5	666	520.2	0.781	0.59	4.84	4.01	43.9	179	93	0.092	0.26	0.19	10.7	2.69	7.16	4.07
(Gh2)	5	551	406.7	0.738	0.58	4.58	3.76	38.1	141	90	0.097	0.21	0.19	10.2	2.57	6.12	3.70
(Gh3)	5	898	655.2	0.729	0.77	5.25	4.41	62.2	224	147	0.057	0.13	0.15	17.2	4.31	6.10	3.60
(Gh4)	5	582	445.2	0.764	0.77	4.81	3.99	50	150	99	0.06	0.19	0.15	16.6	4.16	5.87	3
(Gh5)	5	269	158.5	0.589	0.61	3.79	3.00	16.9	60	43	0.210	0.40	0.29	4.76	1.19	6.25	3.55
(Gh6)	4	73	65.9	0.902	0.63	3.97	3.18	15.8	21	34	0.084	0.22	0.18	11.8	2.97	2.14	1.32
(Gh7)	5	136	77	0.566	1.77	3.40	2.65	14.3	33	12	0.161	2.87	0.25	6.19	1.54	11.3	2.30
Garf	6	554	392.8	0.709	0.46	3.54	2.78	31.35	135	77	0.137	0.28	0.23	7.28	1.82	7.19	4.30

(U) Number of orders; (N_u) Stream number; (L_u) stream length; (L_{sm}) mean stream length; (R_L) Stream length ratio; (R_b) Bifurcation ratio; (R_{bm}) Mean bifurcation ratio; (L_p) basin length; (A) basin area; (P) perimeter; (R_f) Form factor (ratio); (R_c) circularity ratio; (R_e) elongation ratio; (B_s) Shape factor; (k) Lemniscate ratio; (D_t) Drainage texture; (B_w) Basin width

Each type of data's quantitative values should be assigned a different score on a scale based on the significance of the flood or risk (Table 5). The impacted zones would then be assessed using the total of the scores by an overlay operation, giving each region a score that reflects the likelihood of a flood. The relationship between parameter values and flash flood risk is used to estimate each parameter using a simple statistical procedure (Pradhan 2010; Youssef et al. 2011). Each parameter is classified into three classes based on morphometric characteristics and their possible degree of risk relationships (Fig. 6). The

calculation used is (Max–Min)/3. Then, the parameters are classified into three intervals as shown in Table 5.

Different scores on a scale are given to achieve a final assessment of flood risks according to their relevance to flood risk. An overlay procedure would analyze the intersected regions by summing up scores to classify each region by a score measure. The outcome is broken down into three groups (low, medium, and high risk) using equal intervals to provide a simple final map. The results are graded on a scale of 1 to 3, in ascending order of hazard importance. For each function, the raw score is normalized using the

Table 4 Drainage texture and relief characteristics morphometric parameters of basins and related sub-basins in RG area

Basin name and related sub-basins codes	Drainage Texture					Relief Characteristics				
	F	D	D_i	L_o	F_n	H_{max}	H_{min}	H	R_r	R_n
Hawashiya (H)	4.004	8.957	0.447	0.055	35.86	842	9	833	6.868	7.461
(H1)	4.088	2.840	1.439	0.176	11.61	829	593	236	4.991	0.670
(H2)	4.174	2.695	1.548	0.185	11.24	832	600	232	6.060	0.625
(H3)	4.088	2.735	1.494	0.182	11.18	797	605	192	7.242	0.525
(H4)	4.259	2.550	1.670	0.196	10.86	869	542	327	15.53	0.834
(H5)	3.733	2.616	1.427	0.191	9.769	927	396	531	19.05	1.389
(H6)	4.020	2.587	1.553	0.193	10.40	814	561	253	13.42	0.654
Hawashiya 2	3.670	2.926	1.254	0.170	10.74	762	4	758	15.87	2.218
Bakr 1	3.447	3.062	1.125	0.163	10.55	841	3	838	17.21	2.566
Bakr 2	3.543	3.058	1.158	0.163	10.84	322	5	317	10.29	0.969
Bakr 3	3.484	3.045	1.144	0.164	10.61	603	5	598	12.21	1.821
AbuHad(AH)	3.941	2.709	1.454	0.184	10.67	944	7	937	10.45	2.539
(AH1)	4.126	2.629	1.569	0.190	10.85	929	556	373	12.07	0.980
(AH2)	4.135	2.626	1.574	0.190	10.85	825	536	289	14.67	0.758
(AH3)	4.428	2.681	1.651	0.186	11.87	829	498	331	15.83	0.887
(AH4)	3	2.572	1.539	0.194	10.18	700	512	188	17.73	0.483
(AH5)	4.714	2.921	1.613	0.171	13.77	698	487	211	32.46	0.616
(AH6)	4.337	2.493	1.739	0.200	10.81	823	524	299	13.71	0.745
(AH7)	4.333	2.513	1.724	0.198	10.89	816	451	365	31.19	0.917
(AH8)	3.827	2.668	1.434	0.187	10.21	760	461	299	15.17	0.798
(AH9)	3.777	2.694	1.402	0.185	10.17	687	482	205	22.28	0.552
(AH10)	3.642	2.685	1.356	0.186	9.783	672	397	275	20.52	0.738
(AH11)	3.210	3.242	0.990	0.154	10.40	494	240	254	15.77	0.823
Gharib(Gh)	3.940	2.888	1.364	0.173	11.38	911	7	904	14.50	2.611
(Gh1)	3.720	2.906	1.280	0.172	10.81	1199	9	1190	27.10	3.458
(Gh2)	3.907	2.884	1.354	0.173	11.27	1196	7	1189	31.20	3.429
(Gh3)	4.008	2.925	1.370	0.170	11.72	903	10	893	14.35	2.612
(Gh4)	3.88	2.968	1.307	0.168	11.51	737	16	721	14.42	2.139
(Gh5)	4.483	2.641	1.697	0.189	11.84	907	599	308	18.22	0.813
(Gh6)	3.476	3.138	1.107	0.159	10.90	399	143	256	16.20	0.803
(Gh7)	4.121	2.333	1.766	0.214	9.616	1052	599	453	31.67	1.057
Garf	4.103	2.963	1.410	0.171	11.94	281	5	276	8.803	0.803

(F) Stream frequency; (D) Drainage density; (D_i) Drainage intensity; (F_n) Infiltration number; (L_o) Overland flow; (H_{max}) Maximum elevation; (H_{min}) Minimum elevation; (H) Basin relief; (R_r) Relief ratio; (R_n) Ruggedness number

equation and considering the different parameter signs. The probability of flooding of the study region is calculated by equation according to morphometric parameters of the RG basins (Table 6):

Flooding Risk = sum of all morphometric parameters illustrated in table 6

$$(Nu + Lu + Lsm + \ldots \ldots .etc).$$

Using this equation, the research region can be classified into three flood hazard susceptibility classes, as seen in the final risk map (Fig. 7). According to the final flood hazard risk map for RG basins, 29% of the RG region's basins and sub-basins are at high risk of flooding. The majority of these sub-basins drain into higher-order basins such as W. Hawashiya. In 46% of the basins and subbasins, the risk of flooding is moderate. Only about a quarter of the basins and sub-basins face a low risk of flooding (Table 7). Most of the high-potential risk basins are concentrated in W. Hawashiya, especially at number H1, H2, and H4 sub-basins. Also, high risk occurs in W. Gharib and W. Garf basins. The fifteen Basins and sub-basins are considered to have moderate flood risk, these basins are W, Abu Had, W. Bakr 2, W. Hawashiya 2, H3, H5, H6, Gh1, Gh2, Gh3, Gh4, AH1, AH2, AH3, AH6, and AH7. In contrast, eight basins and sub-basins have a low risk of flooding (Fig. 7).

Table 5 Score assigned for morphometric parameters in RG basins and its related sub-basins

Parameter		Flood Probability	Attribute		Raw Score
			Main basins	Sub-basins	
1	Stream number (N_u)	Low	< 552	< 377	1
		Medium	552–700	377–703	2
		High	> 700	> 703	3
2	Stream length (L_u) km	High	< 457	< 246.7	3
		Medium	457–566	246–455	2
		Low	> 566	> 455.7	1
3	Mean stream length (L_{sm}) km	High	< 0.76	< 0.713	3
		Medium	0.76–0.83	0.713–0.86	2
		Low	> 0.83	> 0.86	1
4	Stream length ratio (R_L)	Low	< 0.79	< 0.58	1
		Medium	0.79–1.12	0.58–0.69	2
		High	> 1.12	> 0.69	3
5	Bifurcation ratio (R_b)	High	< 4.23	< 3.76	3
		Medium	4.23–4.91	3.76–4.83	2
		Low	> 4.91	> 4.83	1
6	Mean bifurcation ratio (R_{bm})	High	< 3.43	< 3	3
		Medium	3.43–4.08	3–4.03	2
		Low	> 4.08	> 4.03	1
7	Basin length (L_b) km	High	< 61	< 25	3
		Medium	61–91	25–43.5	2
		Low	> 91	> 43.5	1
8	Basin area (A) km^2	Low	< 533	< 91.6	1
		Medium	533–952	91.6–169.2	2
		High	> 952	> 169.2	3
9	Basin perimeter (P) km	Low	< 158	< 49	1
		Medium	158–251	49–86	2
		High	> 251	> 86	3
10	Form factor (ratio) (R_f)	Low	< 0.113	< 0.148	1
		Medium	0.11–0.17	0.148–0.23	2
		High	> 0.176	> 0.239	3
11	Circularity ratio (R_c)	Low	< 0.23	< 0.266	1
		Medium	0.23–0.33	0.266–0.40	2
		High	> 0.33	> 0.402	3
12	Elongation ratio (R_e)	High	< 0.203	< 0.22	3
		Medium	0.20–0.25	0.22–0.29	2
		Low	> 0.256	> 0.29	1
13	Shape factor (B_s)	High	< 9.1	< 7.74	3
		Medium	9.1–14	7.74–12.47	2
		Low	> 14	> 12.47	1
14	Lemniscate ratio (k)	High	< 2.28	< 1.93	3
		Medium	2.28–3.51	1.93–3.11	2
		Low	> 3.51	> 3.11	1
15	Drainage texture (D_t)	Low	< 10.08	< 4.4	1
		Medium	10.0–16.2	4.4–7.2	2
		High	> 16.24	> 7.2	3
16	Basin width (B_w) Km	Low	< 6.64	< 3.32	1
		Medium	6.64–10.7	3.32–5.6	2
		High	> 10.7	> 5.6	3

Table 5 (continued)

Parameter		Flood Probability	Attribute		Raw Score
			Main basins	Sub-basins	
17	Stream frequency (F)	Low	<3.67	<3.571	1
		Medium	3.67–3.89	3.57–4.14	2
		High	>3.89	>4.142	3
18	Drainage density (D) km/km^2	Low	<2.83	<2.636	1
		Medium	2.83–2.95	2.63–2.93	2
		High	>2.95	>2.939	3
19	Drainage intensity (D_i)	Low	<0.78	<1.248	1
		Medium	0.78–1.11	1.24–1.50	2
		High	>1.11	>1.506	3
20	Length of overland flow (L_o) km	High	<0.1	<0.174	3
		Medium	0.1–0.14	0.174–0.19	2
		Low	>0.14	>0.194	1
21	Infiltration number (F_n)	Low	<11.04	<10.36	1
		Medium	11.0–11.5	10.36–11.1	2
		High	>11.52	>11.11	3
22	Basin relief (H)	Low	<497	<302	1
		Medium	497–718	302–416	2
		High	>718	>416	3
23	Relief ratio (R_r)	Low	<10.32	<14	1
		Medium	10.3–13.7	14–23	2
		High	>13.77	>23	3
24	Ruggedness number (R_n)	High	<1.41	<1.033	3
		Medium	1.41–2.02	1.03–1.58	2
		Low	>2.02	>1.583	1

Runoff potentiality mapping

Storm events in Egypt's Eastern Desert typically last from less than an hour to several hours and are of high intensity (Egyptian Geological Survey and Mining Authority 1994). These storm events frequently cause severe flash flooding, causing serious disruption and significant loss of human lives and property. These flash floods are the result of a complicated natural occurrence, but their causes can be understood by looking at how topographic features and meteorological extremes interact to promote flooding (Komuscu et al. 1998). Water that has not been abstracted from the storm events' incoming precipitation leaves the watershed as surface runoff. Discharge is the amount of runoff that occurs at any given time, measured in terms of volume per unit of time. The peak discharge of runoff has been a focus of flooding studies (Papp 2002). Surface runoff has been studied for a long time and suggested and developed some sophisticated theories and methods for estimating flood flows. At best, most attempts to explain the process were only marginally successful, owing to the difficulty of this process. It should be noted that there is no precise process, which means that

different widely used approaches may produce dramatically different results in a specific location (NHI 2002).

The peak discharge (Qp) and the time of peak (tp) are estimated for each basin and related sub-basins. The obtained data are listed in Table 8. The results show that the average peak discharges of RG basins ranged from 35.9 m3/sec to 220.7 m3/sec and the highest values of peak discharge were recorded at W. Gharib basin (220.7 m3/sec), W. Hawashiya (182.8 m3/sec), W. Abu Had (137.2 m3/sec) and W. Hawashiya 2 (65.5 m3/sec). Whereas the results values of peak discharge for 24 sub-basins ranged from 11 m3/sec to 92.9 m3/sec and the highest values of peak discharge were recorded at W. H1, W. H2, W.H5, W. Gh1, W. Gh2, W. Gh3, W. Gh4, W. AH1 and W. AH2 (Table 8).

The moderate values of peak discharge were recorded at the W. Garf basin (47.7 m3/sec) and W. H3, H4, and AH6 sub-basins, while the low values were recorded at W. Bakr 1 basin (42.6 m3/sec), W. Bakr 2 basin (41 m3/sec), W. Bakr 3 basin (35.9 m3/sec) and W. H6, Gh5, Gh6, Gh7, AH3, AH4, AH5, AH7, AH8, AH9, AH10, AH11 sub-basins. Due to the scarcity of field runoff measurements, empirical or conceptual mathematical formulas are used
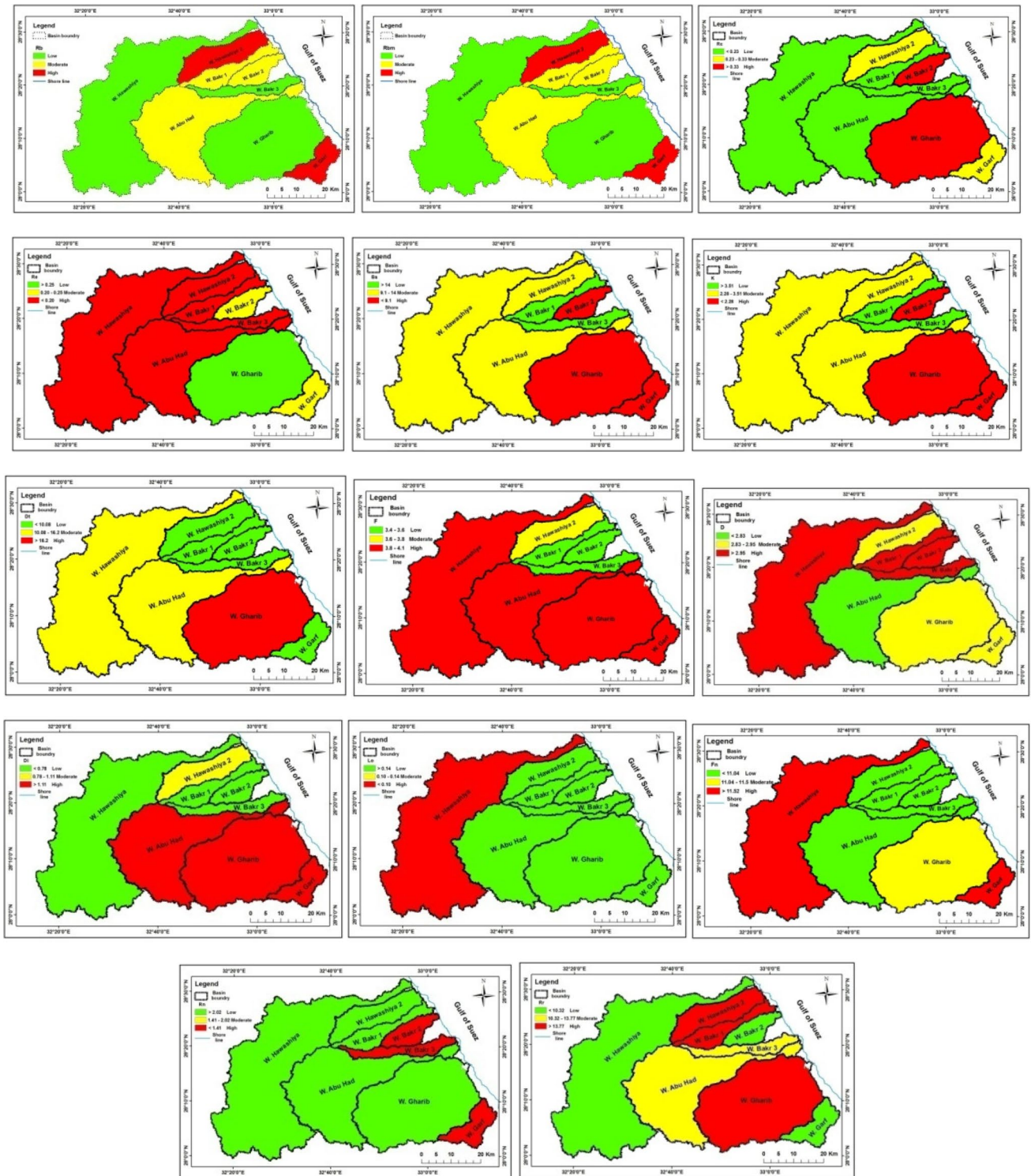
Fig. 6 Calculated morphometric parameters for RG area basins drainage networks

to estimate the peak discharge and peak time for the studied basins. Due to their large utilization and easily available input requirements, the estimated maximum value of runoff and synthetic unit hydrographs has been assumed

here. Clearly, these methods are estimates but can be used as flood risk predictors. Two synthetic unit hydrographs were used to estimate the risk levels of the watershed's basins and sub-basins. Peak discharge and peak time are

Table 6 Flash flood hazard weight numbers of the RG drainage basins and related sub-basins

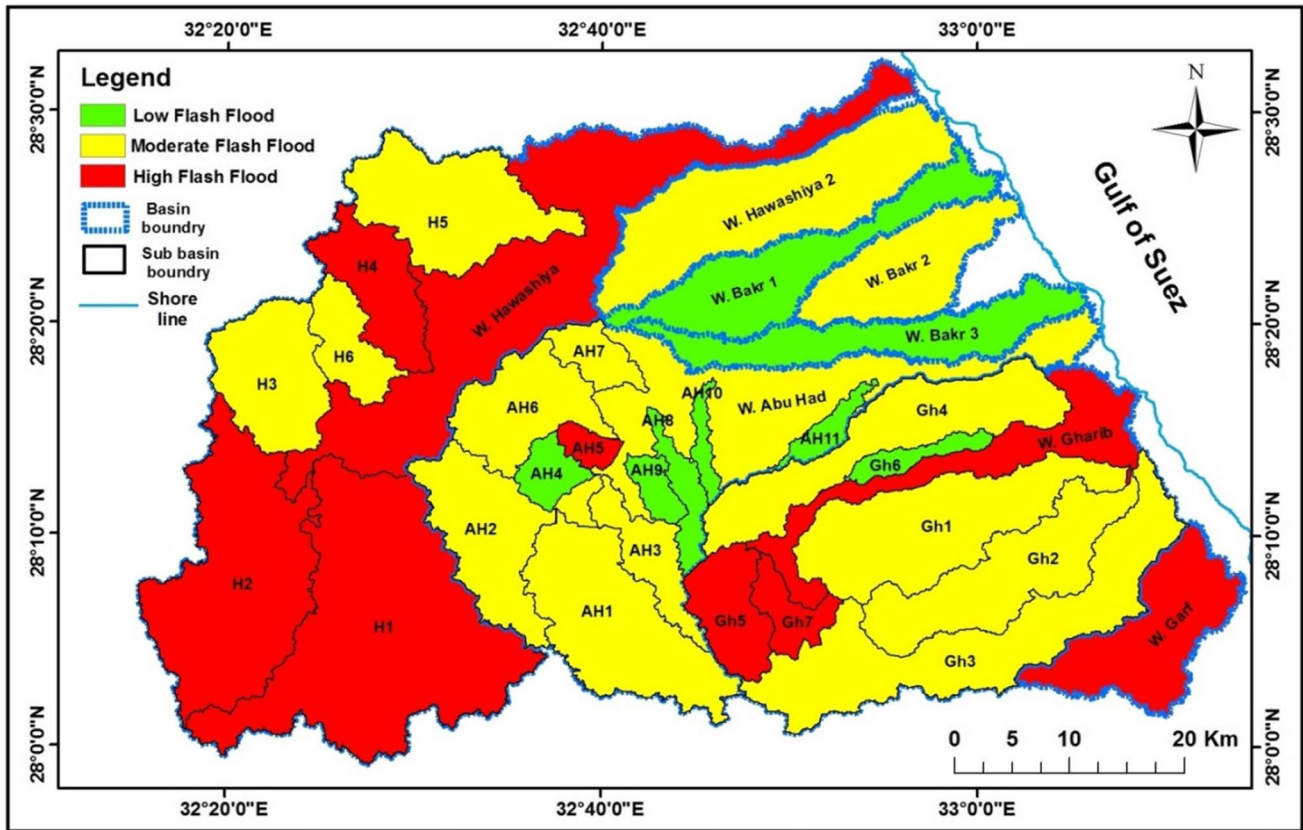| Name Basin		Scores based on the morphometric parameters																								Total Hazard
		N_u	L_u	L_{sm}	R_l	R_b	R_{bm}	L_b	A	P	R_f	R_c	R_e	B_s	K	D_t	B_w	F	D	D_i	L_o	F_n	H	R_r	R_n	
Hawashiya(H)		3	1	1	3	1	1	1	3	3	1	1	3	2	2	2	3	3	3	1	3	3	3	1	1	49
Hawashiya Sub-basins	(H1)	3	1	3	1	2	2	1	3	3	2	1	2	3	3	3	3	2	2	2	2	3	1	1	3	52
	(H2)	3	1	3	1	2	2	2	3	3	2	1	2	3	3	3	3	3	2	3	2	3	1	1	3	55
	(H3)	2	2	3	1	2	2	2	2	2	1	3	2	3	3	3	2	2	2	2	2	3	1	1	3	51
	(H4)	1	3	3	2	2	2	3	1	2	2	2	2	3	3	2	2	3	1	3	1	2	2	2	3	52
	(H5)	2	2	3	1	2	2	2	2	2	2	2	2	3	3	2	2	2	1	2	2	1	3	2	2	49
	(H6)	1	3	3	1	3	3	3	1	1	1	2	2	3	3	2	1	2	1	3	2	2	1	1	3	48
Hawashiya 2		3	1	2	1	3	3	3	1	1	1	2	3	2	2	1	1	2	2	1	2	1	3	3	1	45
Bakr 1		1	3	1	2	2	2	3	1	1	1	2	3	1	1	1	1	1	3	1	3	1	3	3	1	39
Bakr 2		1	3	1	1	2	2	3	1	1	2	3	2	3	3	1	1	1	3	1	1	1	1	1	3	42
Bakr 3		1	3	1	1	1	1	3	1	1	1	1	3	1	1	1	1	3	3	1	1	1	2	2	2	35
AbuHad(AH)		3	1	3	1	2	2	2	3	2	1	1	3	2	2	2	2	3	1	3	1	1	3	2	1	47
Abu Had Sub-basins	(AH1)	2	2	3	1	1	1	2	2	3	2	2	2	3	3	3	2	2	2	3	2	2	2	1	3	50
	(AH2)	2	2	3	1	2	2	3	2	2	3	2	1	3	3	3	3	2	1	3	2	2	1	2	3	51
	(AH3)	1	3	3	2	1	1	3	1	2	1	1	3	2	2	1	1	3	2	3	2	3	2	2	3	48
	(AH4)	1	3	3	1	2	2	3	1	1	2	3	1	3	3	1	1	1	1	3	2	1	1	2	3	45
	(AH5)	1	3	3	1	3	3	3	1	1	3	3	3	3	3	2	1	3	2	3	3	3	1	3	3	55
	(AH6)	2	3	3	2	2	2	3	2	2	2	2	2	3	3	2	2	3	1	3	1	2	1	1	3	51
	(AH7)	1	3	3	2	2	2	3	1	2	2	2	2	3	3	3	1	3	1	3	2	2	2	3	3	50
	(AH8)	1	3	3	3	2	2	3	1	1	1	1	3	1	1	2	1	2	2	2	2	1	1	2	3	43
	(AH9)	1	3	2	2	2	2	3	1	1	2	2	2	3	3	1	1	2	2	2	2	1	1	2	3	46
	(AH10)	1	3	2	3	3	3	3	1	1	1	1	3	1	3	1	1	2	2	2	3	2	1	2	3	44
	(AH11)	1	3	1	3	2	3	3	1	1	1	1	3	1	1	1	1	1	3	1	3	2	1	2	3	43
Gharib(Gh)		3	1	3	1	1	1	2	2	2	3	3	1	3	3	3	3	3	2	3	1	2	3	3	1	53
Gharib Sub-basins	(Gh1)	2	1	2	2	1	2	1	3	3	1	2	3	2	2	2	2	2	2	2	3	2	3	3	1	49
	(Gh2)	2	2	2	2	2	2	2	2	3	1	1	3	2	2	2	2	2	2	2	3	3	3	3	1	51
	(Gh3)	3	1	2	3	1	1	1	3	3	1	1	3	1	2	2	2	2	2	2	3	3	3	3	1	47
	(Gh4)	2	2	2	3	2	2	1	2	3	1	1	3	1	2	2	1	2	3	2	3	3	3	2	1	48
	(Gh5)	1	3	3	2	2	2	3	1	1	3	2	2	3	3	2	2	3	2	3	2	3	2	2	3	55
	(Gh6)	1	3	1	2	2	2	3	1	1	1	1	3	2	2	3	1	1	3	1	3	2	1	1	3	43
	(Gh7)	1	3	3	3	3	3	3	1	2	2	2	2	3	3	3	1	2	1	3	1	1	3	3	2	53
Garf		2	3	3	1	3	3	3	1	1	2	2	2	3	3	1	3	3	2	3	1	3	1	1	3	51

Fig. 7 Flood hazard risk susceptibility map based on morphometric parameters for RG basins and sub-basins

Table 7 Integrated flood risk scores for basins and sub-basins of RG area

Class	Risk	Total score of parameter		Percent	Basins
		Basins	Sub-basins		
1	Low	<41	<47	25	Bakr1, Bakr3, Gh6, AH4, AH8, AH9, AH10, AH11
2	Medium	41–47	47–51	46	AH, Bakr2, Hawashiya2, H3, H5, H6, Gh1, Gh2, Gh3, Gh4, AH1, AH2, AH3, AH6, AH7
3	High	>47	>51	29	H, Gh, Garf, H1, H2, H4, Gh5, Gh7, AH3

calculated for each method (Snyder and SCS) and the average of these parameters is given. Peak discharge and peak time are estimated using a simple statistical method based on the relationship between parameter values and runoff probability (Pradhan 2010; Youssef et al. 2011). Each parameter is divided into three groups based on the possible degree of risk related to each. The used formula is (Max–Min)/3. Then, as shown in Table 9, the parameters are divided into 3 intervals. The outcome is broken down into three groups (low, medium, and high risk) using equal intervals to provide a simple final map. The results

are graded on a scale of 1 to 3, in ascending hazard significance order (Table 10). The raw score of each feature is normalized using an equation that takes into account the various parameter signs. The cumulated runoff risk of the study area according to peak discharge and peak time parameters of the RG basins is estimated by the equation:

Cumulated runoff risk rating = (value of peak discharge ∗ score)

+ (value of time to peak ∗ score)

According to this equation, the study area could be divided into three classes of runoff hazard susceptibility,

Table 8 Peak discharge (Q_p) and the time of peak (T_p) results of synthetic hydrographs of Snyder and SCS methods of RG basins and related sub-basins, where; T_b: Time base (hr), T_L: Lag time (hr), T_p: Time to peak (hr), L: stream length (mile), L_c: Length along the main stream to the watershed centroid (mile), D: The duration of the rainfall excess (hr), A: Basin area (mile2), Qp: Peak of discharge (m3/s), T_C: Time of concentration (hr), W_s: Average watershed slope (%)

Basin name and related sub-basins codes	Snyder method									SCS method							Q_p & T_p (Avg.)	
	L (mi)	L_c (mi)	T_l (hr)	T_b (hr)	T_p (hr)	D (hr)	A (mi²)	Q_p (Ft/s)	Q_p (m³/s)	T_l (hr)	T_c (hr)	D (hr)	T_p (hr)	Ws %	Q_p (Ft/s)	Q_p (m³/s)	Q_p Avg	T_p Avg
Hawashiya(H)	75.4	45.4	23.0	140.9	25.1	4.2	529.7	8851.9	250.6	50.5	84.3	25.2	63.1	0.7	4063.5	115.0	182.8	44.1
(H1)	29.4	14.0	12.2	108.5	13.3	2.2	144.4	4558.3	129.0	27.9	46.5	13.9	34.8	0.5	2006.3	56.8	92.9	24.1
(H2)	23.8	13.1	11.2	105.6	12.2	2.0	95.4	3269.7	92.6	21.4	35.7	10.7	26.7	0.6	1728.7	48.9	70.8	19.5
(H3)	16.5	6.5	8.1	96.4	8.9	1.5	39.4	1858.7	52.6	14.6	24.3	7.3	18.2	0.7	1047.1	29.6	41.1	13.5
(H4)	13.1	7.0	7.8	95.3	8.5	1.4	29.7	1470.9	41.6	8.3	13.8	4.1	10.3	1.6	1392.2	39.4	40.5	9.4
(H5)	17.3	9.2	9.2	99.5	10.0	1.7	53.7	2251.1	63.7	9.3	15.6	4.7	11.7	1.9	2223.5	62.9	63.3	10.8
(H6)	11.7	6.5	7.3	94.0	8.0	1.3	18.9	989.1	28.0	8.1	13.6	4.1	10.2	1.3	899.5	25.5	26.7	9.1
Hawashiya 2	29.7	22.6	14.1	114.2	15.4	2.6	89.2	2431.9	68.8	15.8	26.3	7.9	19.7	1.6	2192.5	62.1	65.5	17.5
Bakr 1	30.2	17.5	13.1	111.4	14.3	2.4	55.2	1616.3	45.8	15.4	25.7	7.7	19.2	1.7	1391.7	39.4	42.6	16.8
Bakr 2	19.1	11.9	10.2	102.5	11.1	1.9	44.0	1659.8	47.0	13.8	23.0	6.9	17.2	1.0	1237.8	35.0	41.0	14.2
Bakr 3	30.4	14.4	12.4	109.2	13.5	2.3	48.6	1507.6	42.7	18.3	30.6	9.2	22.9	1.2	1027.9	29.1	35.9	18.2
AbuHad(AH)	55.7	37.5	19.8	131.4	21.6	3.6	308.1	5973.6	169.1	32.1	53.6	16.0	40.1	1.0	3716.6	105.2	137.2	30.9
(AH1)	19.2	10.3	9.8	101.3	10.7	1.8	64.1	2518.1	71.3	12.8	21.3	6.4	15.9	1.2	1946.1	55.1	63.2	13.3
(AH2)	12.2	7.3	7.7	95.1	8.4	1.4	42.9	2140.5	60.6	8.1	13.5	4.0	10.1	1.5	2056.4	58.2	59.4	9.2
(AH3)	13.0	7.7	8.0	95.9	8.7	1.4	18.9	912.3	25.8	8.1	13.6	4.1	10.2	1.6	899.6	25.5	25.6	9.4
(AH4)	6.6	3.9	5.3	87.8	5.8	1.0	9.7	702.5	19.9	4.5	7.5	2.2	5.6	1.8	836.1	23.7	21.8	5.7
(AH5)	4.0	2.5	4.0	84.1	4.4	0.7	5.4	515.7	14.6	2.2	3.7	1.1	2.8	3.2	936.8	26.5	20.6	3.6
(AH6)	13.5	7.3	7.9	95.8	8.7	1.4	34.4	1660.7	47.0	9.0	15.1	4.5	11.3	1.4	1470.2	41.6	44.3	10.0
(AH7)	7.3	4.4	5.7	89.0	6.2	1.0	11.6	785.7	22.2	3.6	6.1	1.8	4.6	3.1	1229.6	34.8	28.5	5.4
(AH8)	12.2	6.4	7.4	94.2	8.1	1.3	11.2	581.0	16.4	7.9	13.2	4.0	9.9	1.5	546.5	15.5	16.0	9.0
(AH9)	5.7	3.2	4.8	86.4	5.2	0.9	6.9	556.3	15.7	3.6	5.9	1.8	4.5	2.2	755.7	21.4	18.6	4.8
(AH10)	8.3	4.2	5.8	89.5	6.3	1.1	5.4	356.6	10.1	5.0	8.4	2.5	6.3	2.1	417.6	11.8	11.0	6.3
(AH11)	10.0	6.0	6.8	92.5	7.4	1.2	7.3	413.1	11.7	6.6	11.1	3.3	8.3	1.6	429.0	12.1	11.9	7.9
Gharib(Gh)	38.7	24.4	15.6	118.9	17.0	2.8	357.9	8796.8	249.0	20.4	34.1	10.2	25.5	1.5	6793.9	192.3	220.7	21.3
(Gh1)	27.3	14.8	12.1	108.3	13.2	2.2	69.1	2193.5	62.1	11.3	18.8	5.6	14.1	2.7	2374.5	67.2	64.7	13.6
(Gh2)	23.7	13.1	11.2	105.6	12.2	2.0	54.4	1869.2	52.9	9.4	15.7	4.7	11.7	3.1	2247.8	63.6	58.3	12.0
(Gh3)	38.6	21.2	15.0	116.9	16.3	2.7	86.5	2219.6	62.8	20.5	34.2	10.2	25.6	1.4	1636.4	46.3	54.6	21.0
(Gh4)	31.1	17.0	13.1	111.3	14.3	2.4	57.9	1696.5	48.0	17.1	28.6	8.6	21.4	1.4	1307.8	37.0	42.5	17.9
(Gh5)	10.5	7.0	7.2	93.7	7.9	1.3	23.2	1227.5	34.7	6.4	10.7	3.2	8.0	1.8	1400.6	39.7	37.2	8.0
(Gh6)	9.8	5.0	6.4	91.3	7.0	1.2	8.1	483.1	13.7	6.4	10.7	3.2	8.0	1.6	487.8	13.8	13.7	7.5
(Gh7)	8.9	4.8	6.2	90.6	6.7	1.1	12.7	791.2	22.4	4.2	7.1	2.1	5.3	3.2	1160.9	32.9	27.6	6.0
Garf	19.5	10.4	9.8	101.5	10.7	1.8	52.1	2035.4	57.6	15.1	25.2	7.6	18.9	0.9	1336.1	37.8	47.7	14.8

as shown in the final risk map (Fig. 8). The Runoff hazard risk final map of RG basins shows that the high potential risk basins concentrated in W. Hawashiya, especially at number H1, H2, and H5 sub-basins. Also, high risk occurs in W. Gharib, W, Hawashiya2, and W. Abu Had basins and Gh1, Gh2, Gh3, Gh4, AH1, and AH2 sub-basins. The three sub-basins are considered to have moderate risk, these sub-basins are H3, H4, and AH6; on other hand, there are sixteen basins and sub-basins that have a low risk (Fig. 8).

Geomorphic and topographic potentiality mapping

The key geomorphological units of the RG area are identified and mapped based on the enhanced satellite data results and field observations (Fig. 9). Those geomorphological units are defined as follows: (1) The Rugged mountainous areas at the western part, (2) The Pediments lands between the rugged mountains and the coastal zone, (3) The Tablelands areas on the eastern and western border

Table 9 Score assigned of peak discharge and time to peak parameters in RG basins and its related sub-basins

Parameter		Runoff Probability	Attribute		Raw Score
1	Peak discharge (Q_p)	Low	< 97.5	< 38.3	1
		Medium	97.5–159	38.3–65.6	2
		High	> 159	> 65.6	3
2	Time to peak (T_p)	High	< 24.1	< 10.4	3
		Medium	24.1–34.1	10.4–17.2	2
		Low	> 34.1	> 17.2	1
3	Cumulated runoff risk	Low	< 94.9	< 75.3	1
		Medium	94.9–106	75.3–120.6	2
		High	> 106.4	> 120.6	3

of the coastal plain or inland occupying the intermountain basins and (4) The Coastal Plain occupies the lowlands parallel to the Red Sea coastline. Using ASTER GDEM data that was adopted and processed, a DEM with a spatial resolution of 29 m was created (Fig. 2). The DEM is regarded as a valuable source of data for obtaining information on various topographical parameters, such as slope and elevation, which contribute to flash floods. The slope is one of the main considerations about the risk of flash flood hazards already occurring. With a spatial resolution of 29 m, we created the slope map using GDEM, divided equally into three groups (Fig. 10). The research area is divided into three classes: 0 to 7; 7 to 20; and > 20. The slope map reveals that places with a gentle slope have a naturally slow surface runoff, which allows precipitation more time to travel and lowers the risk of flooding. On the other hand, places with steep slopes encourage quick surface runoff, which results in less time for precipitation to move and a higher risk of flooding. Due to their steep slope gradients, the southern and central portions of the RG region are more susceptible to flooding than the majority of the eastern portions, which have mild slopes. The path and velocity of the runoff, the severity, and the depth of the flood are all impacted by elevation, making it a crucial aspect in the appropriate assessment of flash flood threats. According to a DEM, the elevation of the RG area varies from 0 to 1687 m. The DEM has divided the study area elevation into three categories (Fig. 11), measuring each category according to its impact on flood incidence. Highland geography is extremely vulnerable to flooding (Bathrellos et al. 2018), while lower-lying terrain is less prone to flood. Areas with a higher elevation are more susceptible to flooding, as water flows more to lower-lying lands than to lower-elevated areas. Floods are influenced by high elevation, which increases the likelihood of flooding as a result. The south and western parts of the RG area have high flood potentiality due to high

Table 10 Runoff hazard weight numbers of the RG drainage basins and related sub-basins

RG area

| Basin name		Scores based on Qp & Tp		
		Qp	Tp	Cumulated Qp + Tp
Hawashiya(H)		3	1	3
Hawashiya Sub-basins	(H1)	3	1	3
	(H2)	3	1	3
	(H3)	2	2	2
	(H4)	2	3	2
	(H5)	2	2	3
	(H6)	1	3	1
Gharib (Gh)		3	3	3
Gharib Sub-basins	(Gh1)	2	2	3
	(Gh2)	2	2	3
	(Gh3)	2	1	3
	(Gh4)	2	1	3
	(Gh5)	1	3	1
	(Gh6)	1	3	1
	(Gh7)	1	3	1
AbuHad (AH)		2	2	3
Abu Had Sub-basins	(AH1)	2	2	3
	(AH2)	2	3	3
	(AH3)	1	3	1
	(AH4)	1	3	1
	(AH5)	1	3	1
	(AH6)	2	3	2
	(AH7)	1	3	1
	(AH8)	1	3	1
	(AH9)	1	3	1
	(AH10)	1	3	1
	(AH11)	1	3	1
Hawashiya 2		1	3	3
Bakr 1		1	3	1
Bakr 2		1	3	1
Bakr 3		1	3	1
Garf		1	3	1
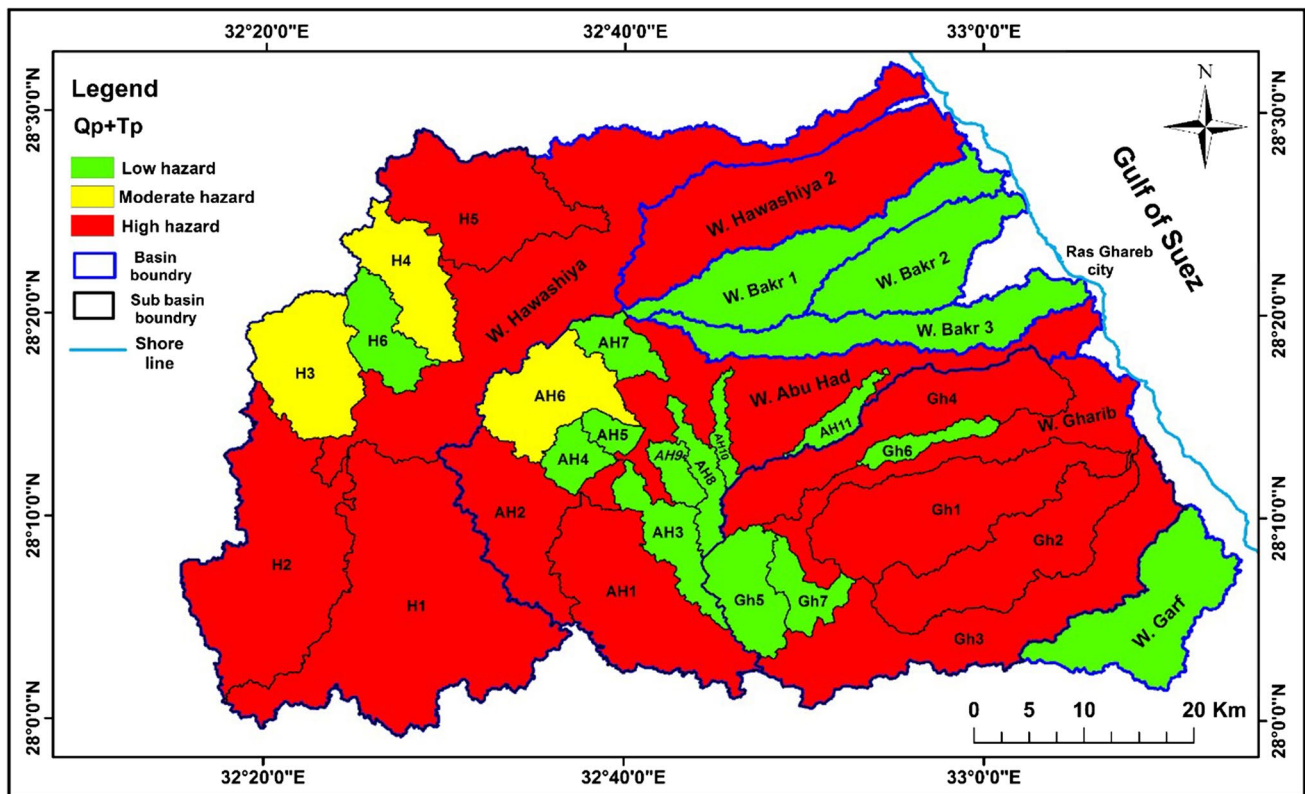
Fig. 8 Cumulative runoff risk map for RG basins and sub-basins

elevation gradients; however, most of the eastern areas have low flood potentiality due to gentle elevation.

Lithology potentiality mapping

The lithological units constitute a critical indicator for assessing flash flood hazard zones. The majority of the Precambrian basement rocks in the RG region underwent significant weathering, making them extremely brittle and prone to disintegration. Additionally, different levels of stress are generated by the structural elements in the studied area, leading to some major weaknesses in the weathered rocks. Weathering of rocks along faults or other structural lineaments, especially on steep slopes, produces an adequate environment to excessive precipitation flowing across weakness lines. Any water that flows along fault lines encourages the abrasion of the disintegrating rocks, which deepens the stream channel as a result. The majority of the studied region is made up of Precambrian basement rocks, while the western, eastern, and middle portions of the mapped area are dominated by Phanerozoic sedimentary rocks, which contain several types of deposits dating from the Paleozoic to the Quaternary (Fig. 12). Because

of their low infiltration capacity, steep slopes, and high relief, Precambrian basement rocks pose a serious risk of flooding. Thus, Precambrian basement rocks, particularly metamorphic rocks, Dokhan Volcanics, and granitoids, have the highest weight value while Quaternary deposits have the lowest weight value (Table 11). Therefore, the locations most vulnerable to sudden floods are those near Precambrian rocks. The final risk map shows three categories of lithological hazard vulnerability that can be matched to the research area (Fig. 13).

Structural lineaments potentiality mapping

The structural lineaments in the study area were expressed as zones of varying lineament densities (lineaments/km2) and classified as high, moderate, and low based on their ability to infiltrate runoff water and their significance in terms of flood hazard potential (Table 12). Flooding is more likely to occur in low-density fracture zones than it is in higher-density fracture zones. Flooding is less likely in zones with a higher-density fracture because water is more likely to infiltrate into the subsurface than in zones with a lower-density fracture. Low fracture density is a major factor in increasing flooding vulnerability. The structural lineament density map
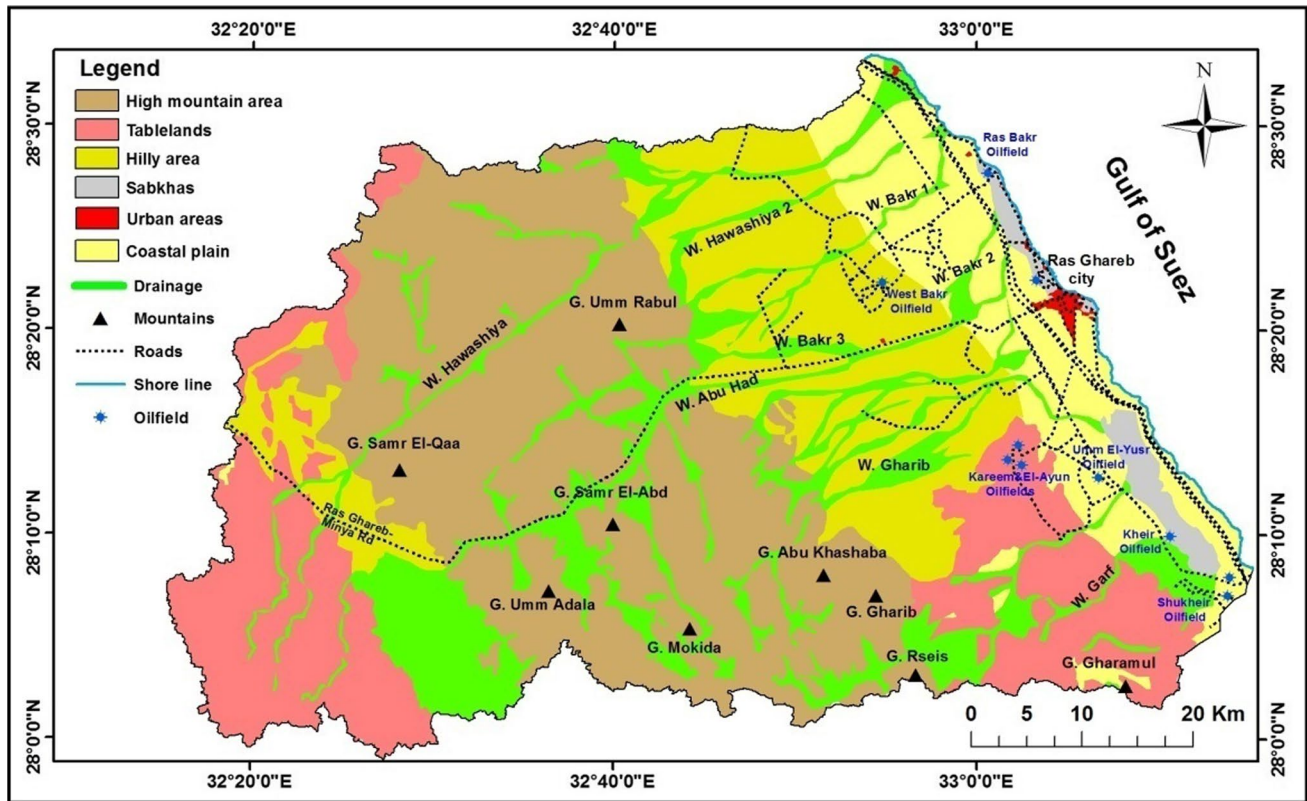
Fig. 9 Geomorphological units of RG area driven from the different enhanced satellite images

(Fig. 14) reveals that the eastern and western zones of the RG region have high flood potential due to low-density fracture; however, most central zones have low flood potential due to high-density fracture.

Runoff volume potentiality mapping

Rainfall is the primary threat factor for flash floods in the study region. Rain causes flooding along the main streams, which primarily flow east and discharge into the Red Sea. Today, data from the Tropical Rainfall Measuring Mission (TRMM) provide valuable information about the effects of rainfall on drainage network systems worldwide. These data are useful in forecasting flash flood risks, as well as estimating surface water runoff volume. Using the satellite products of TRMM 3B42 V7, based on daily data from 1998 to 2018, rainfall estimation is presented in Fig. 15. The spatial resolution is $0.25° \times 0.25°$ (~685 km^2). The expected maximum value of runoff volume for each basin in the study area can be calculated according to the empirical equation, developed by Ball (1937):

$$V = 750\ A\ (R - 8)$$

where V is the probable maximum volume of runoff in m^3, A is the drainage basin area in km^2, and R is the maximum rainfall depth in one day in mm. The TRMM data for the research area was interpolated and classified as low, moderate, and high using ArcGIS (Fig. 15) & (Table 13). The final Rainfall Hazard Risk Map of RG Basins reveals that the high-potential risk basins are localized in W. Hawashiya, W. Abu Had, and W. Gharib. The W. Hawashiya 2 basin is the only one deemed to be at moderate risk (Fig. 16).

Flash flood risk integrated modeling

The present study uses RS and GIS data from the RG region to identify the flood-prone zones. The geospatial techniques were effectively used to categorize and create a geographical distribution map of flood accumulation potential based on numerous influencing factors. Thus, a flash flood potential map was built using a linear combination of these variables in a spatial analysis setting of ArcGIS. Some of the various thematic geospatial maps mentioned in the preceding have been converted into raster form. These were reclassified, and appropriate weights were assigned. Using the specified assessing variables, the levels of flash flood risk in the study
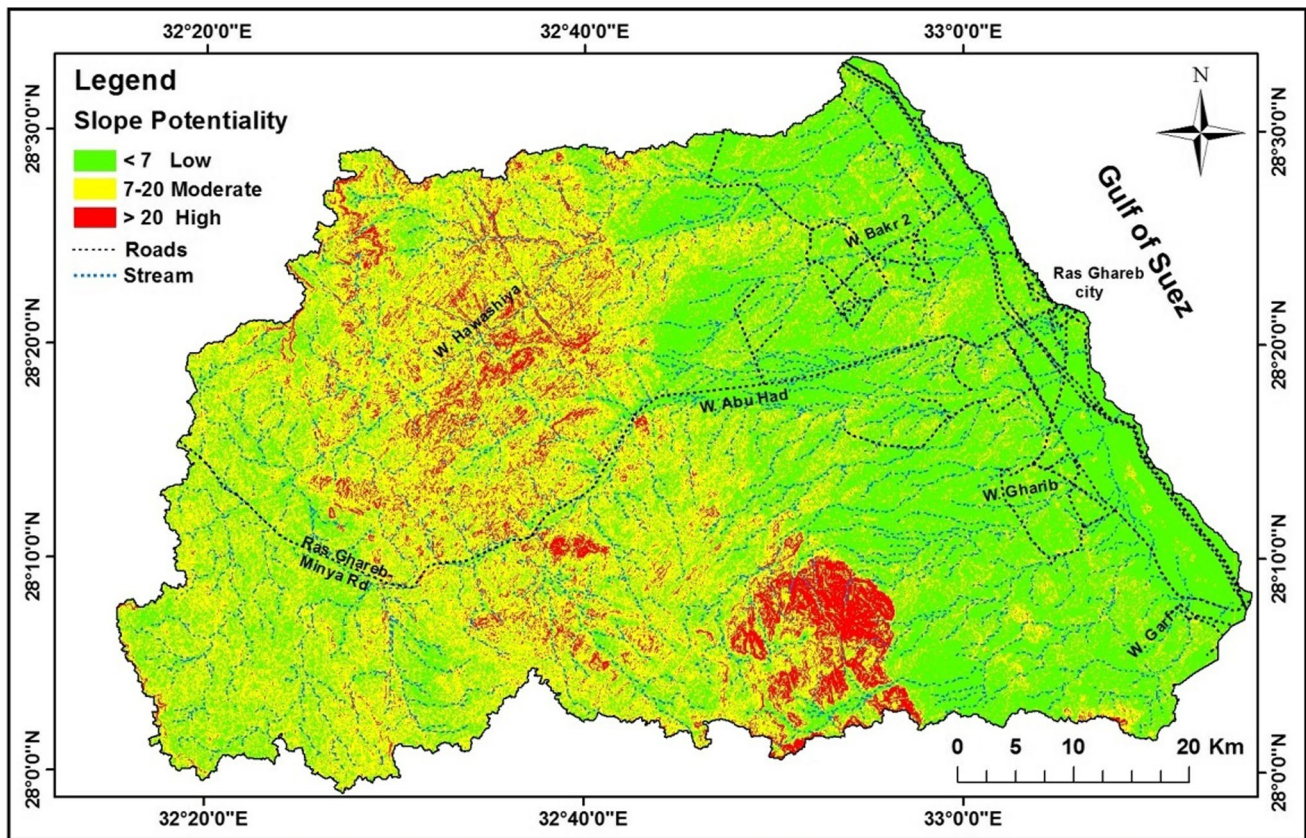
Fig. 10 Flood risk potentiality map based on slope parameters for RG area

area were determined. Seven variables are regarded as new layers incorporated to a model. All of these variables are regarded as equally important and are found all across the study area. These variables are morphometric parameters, cumulated runoff, lithological units, slope degree, elevation, lineament density, and runoff volume. Integrating this data could give the study area the site of high-risk spots. Depending on the severity of a flood or risk, different subjective values associated with various types of data should be assigned different scale scores. An overlay activity will then compare the intersected regions by a sum of the scores, so each region is defined by a score that tests its flood prospect potential. The analysis of each factor is estimated using a simple statistical procedure, based on the relationship between factor values and flash flood risk (Pradhan 2010; Youssef et al. 2011). Each factor is divided into three groups based on the possible degree of risk related to each. The used formula is (Max–Min)/3. Then it classifies the variables into three intervals.

Different scores on a scale are given to achieve a final assessment of flood risks according to their relevance to flood risk. An overlay procedure would analyze the intersected regions by summing up scores in order to classify each region by a score metric. To provide a clear final map, the results are divided into three classes (low, medium, and high risk). The findings are ranked from 1 to 3 on a scale based on the severity of the hazard. The algorithm that takes into account the various parameter signs also normalizes the raw score for each attribute. Based on this integration, the study area can be divided into three classes of flood hazard susceptibility (Table 14), as illustrated in the final risk map (Fig. 17). The final flood hazard risk map for the RG area (Fig. 17) reveals that 62% of the basins and sub-basins in the area are at high risk of flooding. Most of these subbasins discharge into larger basins, like the W. Hawashiya, W. Abu Had, and W. Gharib. Medium risk of flooding exists in 33% of all basins and subbasins. The remainders, or around 5% of the basins and subbasins, are less prone to flooding (Table 14). Most of the high-potential risk basins are concentrated in W. Hawashiya, especially at H1, H2, H3, H4, H5, and H6 sub-basins. Also, high risk occurs in W. Abu Had at AH1, AH2, AH3, AH4, AH5, AH6, and AH7 sub-basins. Also, high risk occurs in W. Gharib at Gh1, Gh2, Gh3, Gh4, Gh5, and Gh7 sub-basins. The ten Basins and sub-basins are considered to have a moderate flood risk.
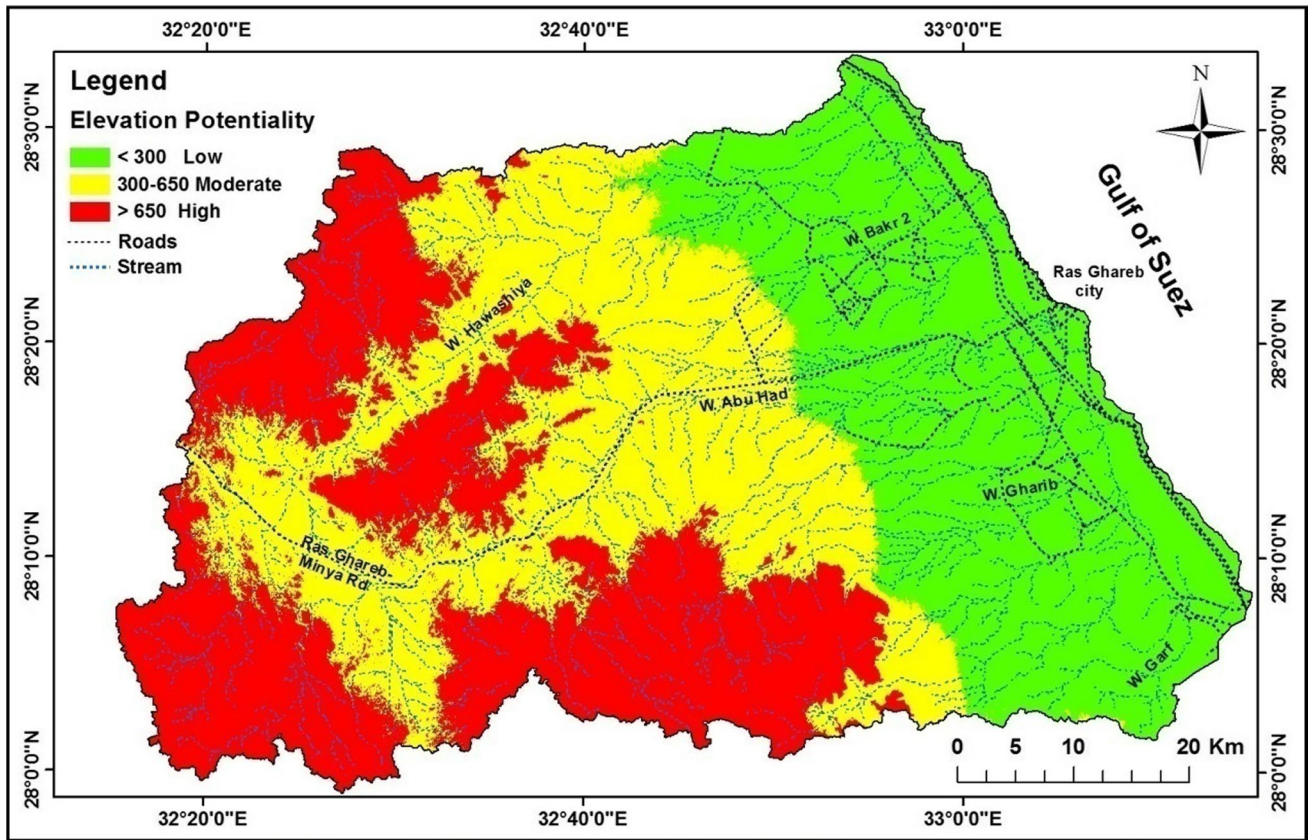
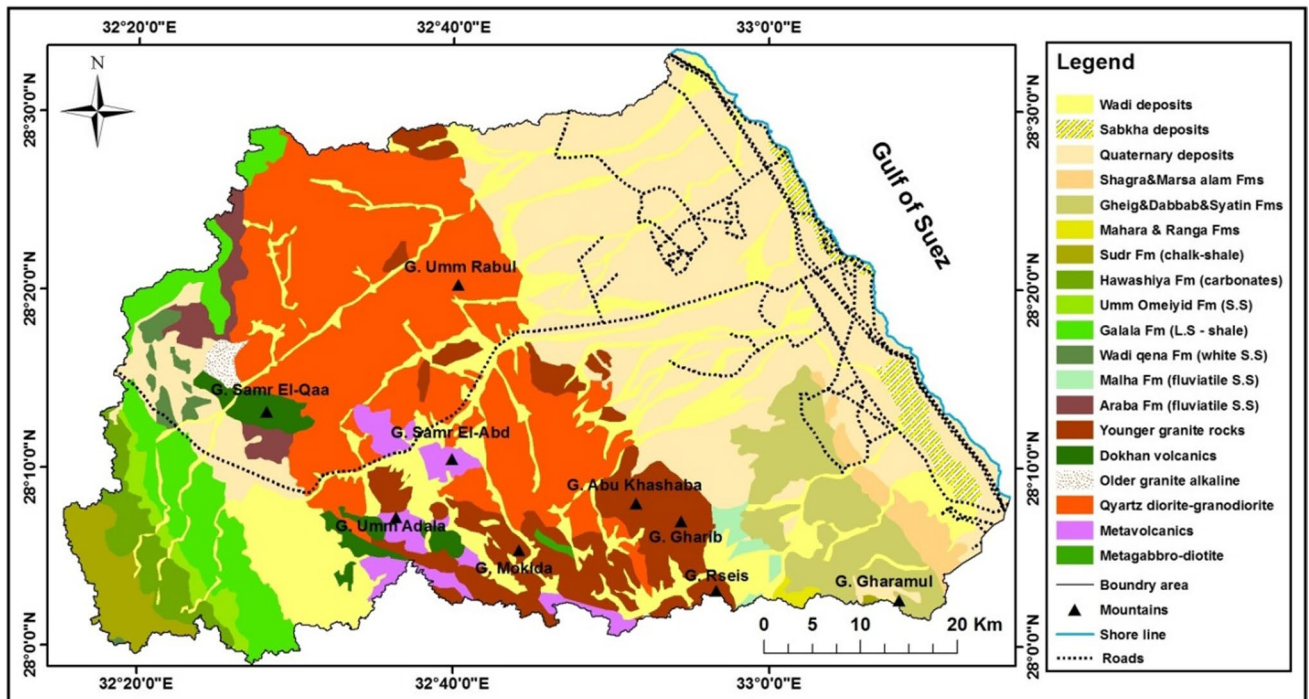**Fig. 11** Flood risk potentiality map based on elevation parameters for RG area

Fig. 12 Lithological map of RG area constructed from the different enhanced satellite images

Table 11 Lithological hazard weight numbers of the Ras Ghareb area

Parameter	flood Probability	Weight
Precambrian igneous and metamorphic rocks	High	3
High fractured igneous rocks and Phanerozoic succession (limestone, chalk, shale, marl)	Moderate	2
Quaternary and recent wadi deposits	Low	1

Model validation and verification

Validation is the task of showing that the model is a fair representation of the real system: that it reproduces system actions with sufficient accuracy to fulfill the goals of the analysis. Although model verification techniques are common, the model validation approach is likely to be far more model-specific and system-specific. In fact, just as model creation is driven by successful study goals, so will the model validation. Typically, a model is designed to address a specific problem, and can therefore represent various parts of the system at various abstraction levels.

Following the occurrence of the flash flood event, the Landsat OLI image for the RG area is compared to the flash flood risk integrated map (Fig. 17). The majority of integrated flash flood risk maps are consistent with Landsat images following a flash flood event, which is one of the results that significantly proved the validity of the model (Fig. 18). It reveals the proper match between the flash flood hazard model and the occurrences of flash flood for some sub-basins (W. H2, W. H4, W. H5, W. AH1, W. AH6, and W. Gh4) in the RG area after the October 27, 2016 rainfall event. The events truth recorded in impacted sites of the RG area confirms the validity of the proposed model based on the October 2016 flash flood event observations (Fig. 19).

Table 12 Structural lineaments hazard weight numbers of the study areas

Class	Risk	structural lineaments density for each grid in RG
3	High	<21
2	Medium	21- 40
1	Low	>40
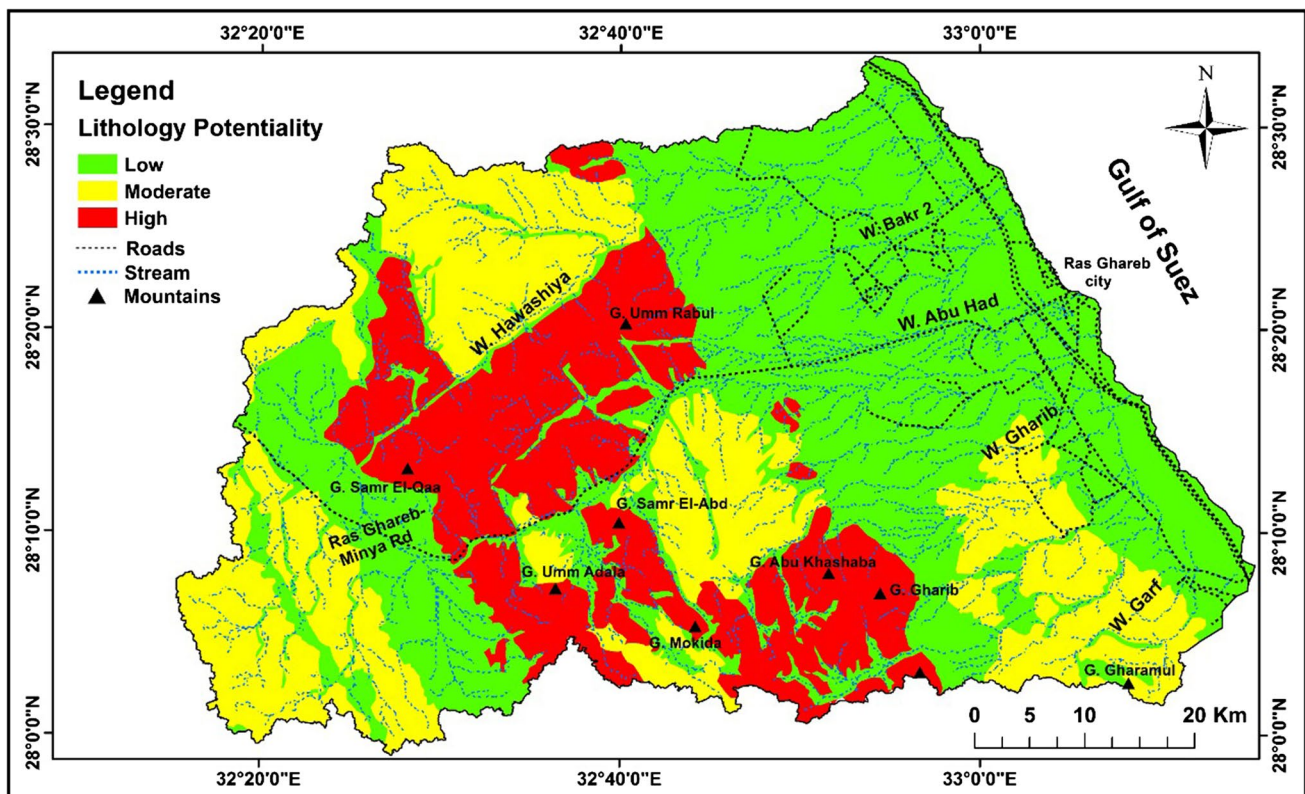
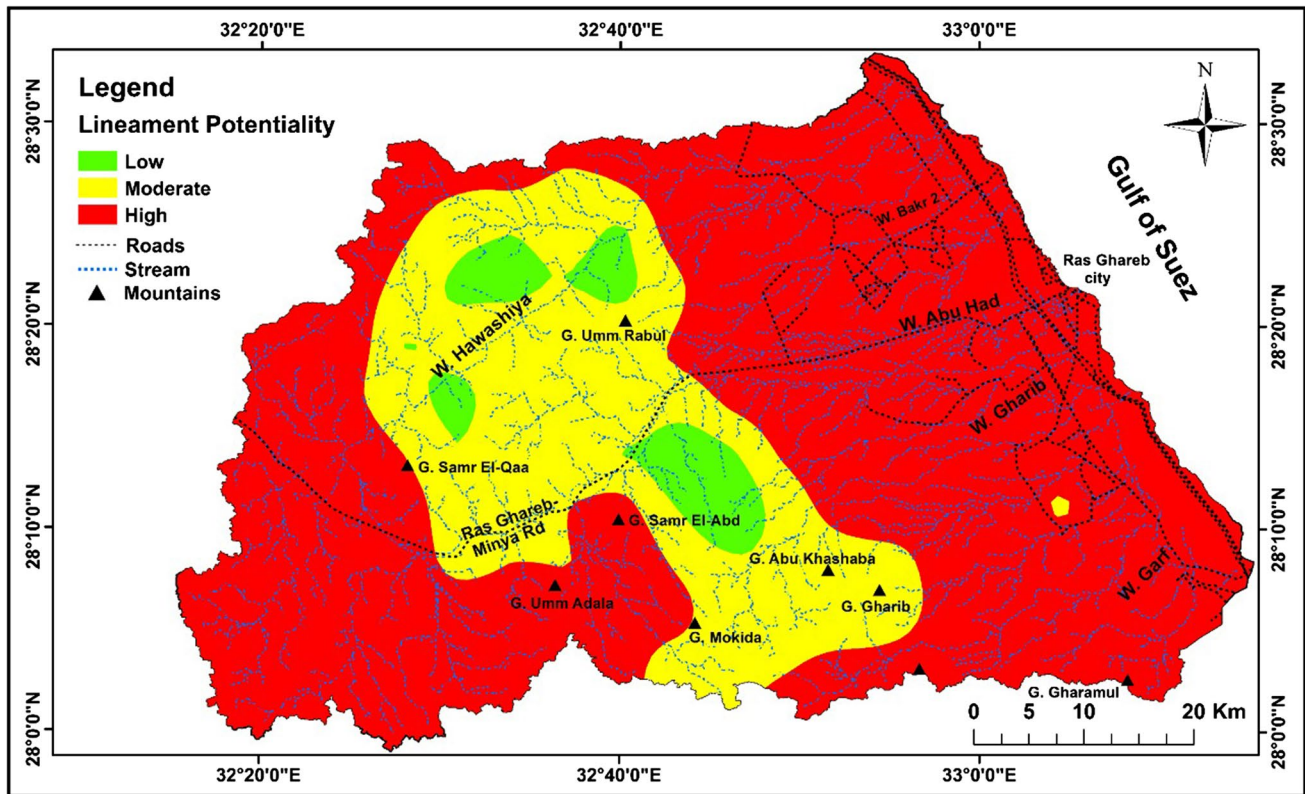**Fig. 13** Flood risk potentiality map based on lithological parameters for RG area

Fig. 14 Flood risk potentiality map based on structural lineaments density for RG area

Flash flood management system

Given the foregoing results of this analytical study of the potential for flash flooding, the present study strongly recommends that flash flood-control measures be made to mitigate the possible flash flood hazards in the study areas. Flash flood management system (Fig. 20) proposes precautionary steps to serve two objectives: one is to reduce flash flood damage and the other is to store and control flood water for domestic purposes, in particular those desert areas experiencing water scarcity. These steps may be structural and nonstructural, and the first should be installed in areas where flash flooding is caused. Common flood control basin-scale has been strongly advocated. During the preparation of the structural steps, consideration should be given to the simplicity, use of indigenous materials, and cost/benefit relation.

Any of the structural steps proposed can be laid down here:

a) Artificial barriers (earth dams), made of cobbles and boulders of Wadi bed deposits without cementation, are recommended in sites covered by impermeable surface soil. The construction of storage dams is proposed to protect threatened sites and store the excess flood water in surface reservoirs and retention basins for future use.

b) To protect the infrastructure of the threatened sites, particularly the main highways, it is recommended that large-enough bridges or culverts be built beneath the roads at the stream crossing sites, or that bridgeless crossing designs be considered during the construction of the threatened roads. Furthermore, to protect the earthen shoulders of roads, it is recommended that suitable local rock materials be used to seal the earthen shoulder body, particularly in highly vulnerable sites.

c) In sites dominated by permeable surface soil, the spreading water technique is recommended to infiltrate surface runoff excess water. This could be accomplished by building retardation dams, which are used to reduce flood water velocity and have a high likelihood of infiltration and rejuvenation of the shallow aquifer. The wide plain to the west of RG City can be used as a floodwater harvesting site in the study areas by spreading floodwater on the floodplain surface, which improves infiltration. Furthermore, building artificial channels (ditches) at right angles to surface flow lines, on narrow steep slopes, and diversion channels at major stream crossings with roads will improve infiltration.

d) Build storage cisterns; another flood-control option is to store floodwater in local surficial reservoirs. The topography of the headwater catchments in the study
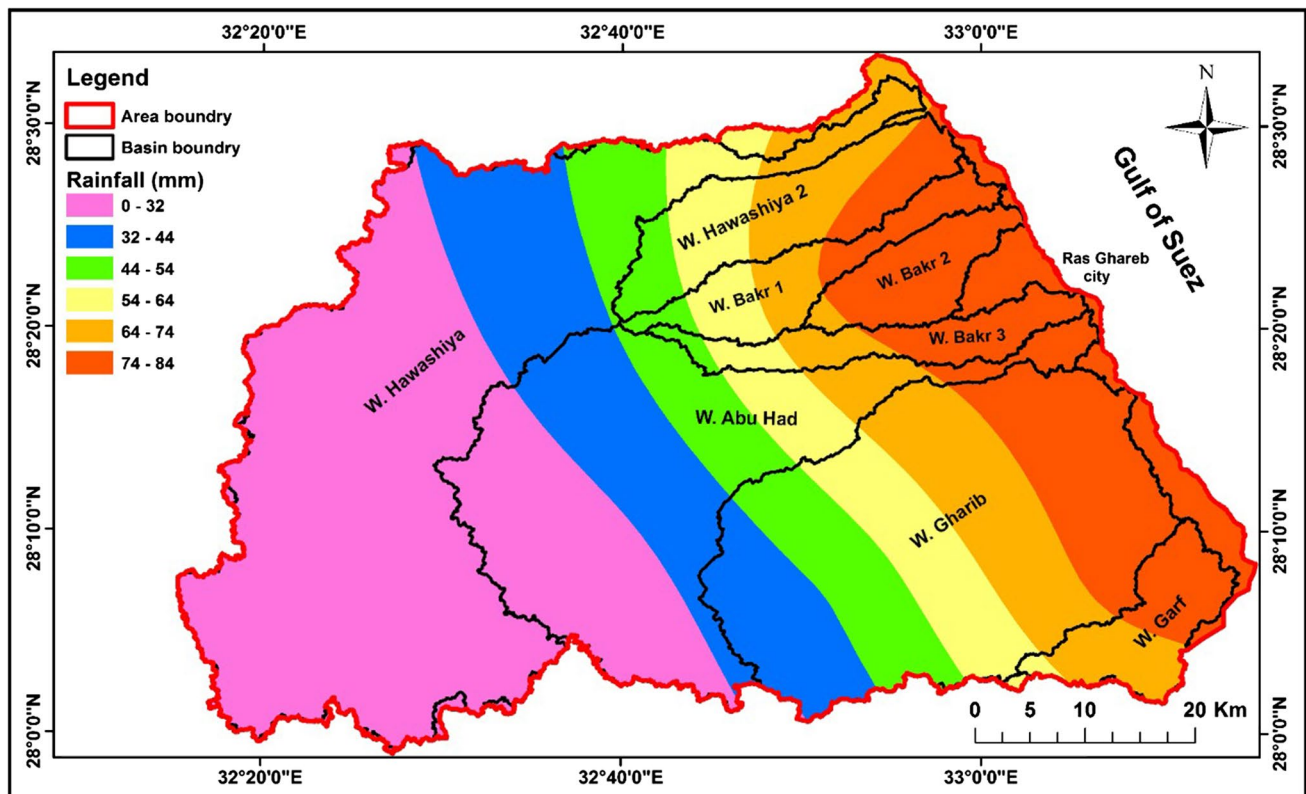
Fig. 15 Spatial distribution of rainfall over the RG basins area from 1988 to 2018

area appears to allow for such construction of reservoirs to store surface runoff water upstream.

e) In addition, the following non-structural implementations are recommended to reduce the impacts of flash flooding:

1) Enforcing the existing regulations and policies prohibiting new construction in flood-prone areas.
2) It is strongly advised to install flood warning systems in vulnerable areas.
3) Raising flash flood hazard awareness among local residents in order to protect themselves from the extreme effects of flooding and to cope with alarm systems.

Table 13 Rainfall volume hazard weight numbers of the study area

Class	Risk	Rainfall volume (*106)	Basins
1	Low	< 7	Hawashiya, Abu Had, Gharib
2	Medium	7–12	Hawashiya2
3	High	> 12	Bakr1, Bakr2, Bakr3, Garf,

Conclusions

Flash flood hazards assessment in the coastal zone of RGC, Red Sea, Egypt was done based on using GIS tools and the spatial multi-criteria approach to assess, integrate, and produce potential flash flood hazard maps. The analytic hierarchy process was utilized to calculate weights of hazard and vulnerability of flash flood controlling factors and their parameters such as topographical, geological, and hydrological factors. In addition to estimating the degree of risk of each individual basin and its sub-basins by combining standardized parameter values. Seven variables were viewed as layers inserted into a flash flood model for the study area. All these variables were believed to be addressed in the entire field of study and were of equal importance. These controlling factors are morphometric parameters, cumulated runoff, lithological units, slope degree, elevation, lineament density, and runoff volume. Integrating this data could give the study area the site of high-risk spots. The quantitative values associated with all kinds of data should have a different score on a scale based on their flood or risk significance. An overlay activity will then compare the intersected regions by a sum of the scores, so each region is defined by a score that tests its flood prospect potential. Therefore, the drainage network and basin boundaries were well defined
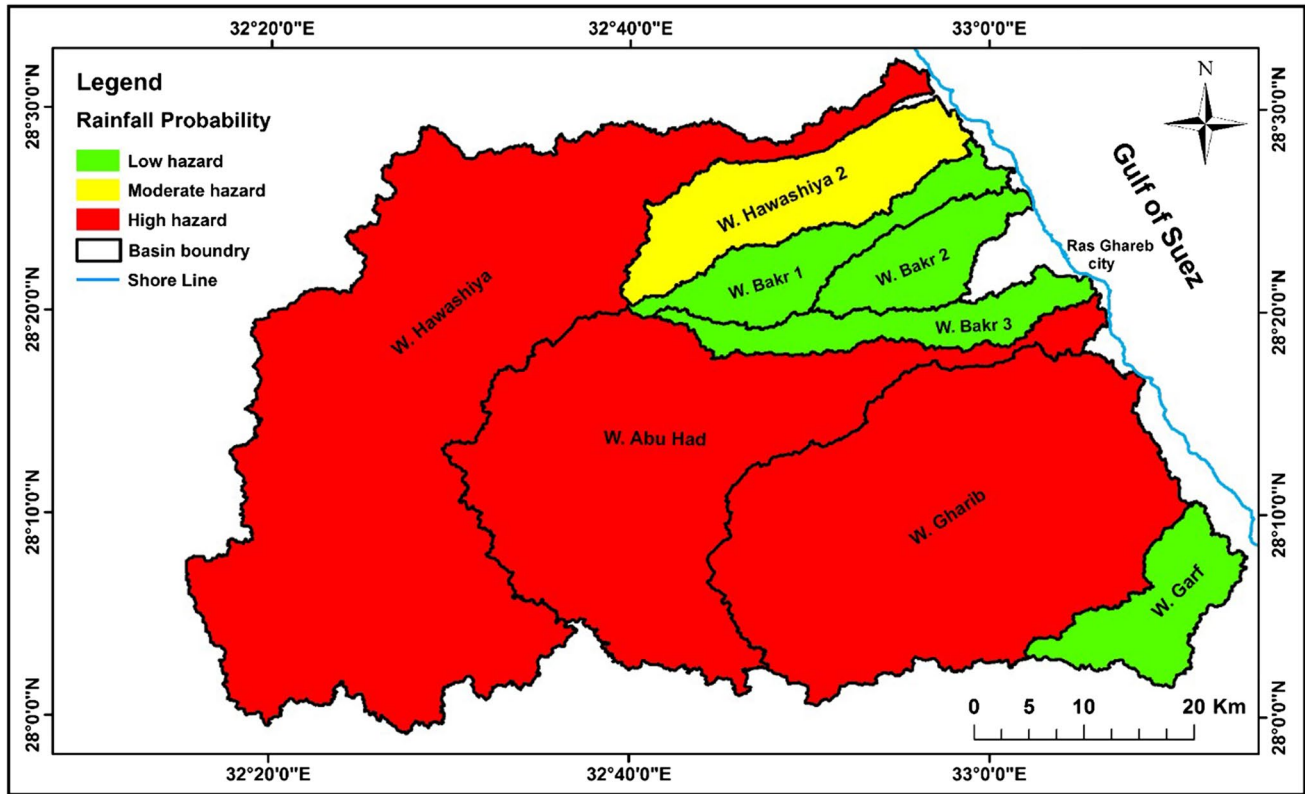
Fig. 16 Flood risk potentiality map based on rainfall probability for RG basins area

and outlined on the correctly enhanced Aster Digital Elevation Model (GDEM) by utilizing ARCHydro tools in the ArcGIS program. In addition, it is compared with reference topographical map sheets of 1: 50,000. RGC sub-basins have been isolated and morphometrically studied to determine vulnerability to flash flooding. In addition, the flash flood threat model was developed using geoprocessing tools provided by ArcGIS software to incorporate all contributing factors spatially. RG area is divided into distinguished eight mega basins; namely Wadi (W.) Hawashiya, W. Hawashiya 2, W. Bakr 1, W. Bakr 2, W. Bakr 3, W Abu Had, W. Gharib and W. Garf. W. Hawashiya is subdivided into six relatively sub-basins; namely H1, H2, H3, H4, H5, and H6. W.Abu Had is sub-divided into eleven relatively sub-basins; namely AH1, AH2, AH3, AH4, AH5, AH6, AH7, AH8, AH9, AH10 and AH11. W. Gharib is subdivided into seven relatively

sub-basins; namely Gh1, Gh2, Gh3, Gh4, Gh5, Gh6, and Gh7. The morphometric parameters of the drainage network were also computed by using the interactivity ArcGIS program. The different types of morphometric parameters were calculated and integrated to create the morphometric parameters potentiality flash hazard map. The flood hazard risk final map of RG basins shows that 29% of the total basins and sub-basins in the RG area have a high flooding risk. Most of these sub-basins are draining into basins of higher order as W. Hawashiya. 46% of all basins and sub-basins have medium flooding risk. The last, about 25%, of the basins and sub-basins have a low-risk flooding susceptibility. Most of the high-potential risk basins are concentrated in W. Hawashiya. Also, high risk occurs in W. Gharib and W. Garf basins. The fifteen Basins and sub-basins are considered to have a moderate flood risk. On other hand, there are eight basins and sub-basins that have a low flooding risk. The results of the runoff show that the average peak discharges of RG basins ranged from 35.9 m3/sec to 220.7 m3/sec and the highest values of peak discharge were recorded at W. Gharib basin (220.7 m3/sec), W. Hawashiya (182.8 m3/sec), W. Abu Had (137.2 m3/sec) and W. Hawashiya 2 (65.5 m3/sec). Whereas the results values of peak discharge for 24 sub-basins ranged from 11 m3/sec to 92.9 m3/sec. The runoff hazard risk final map of RG basins shows that the

Table 14 Scoring of the integrated flood risk potentiality in RG area

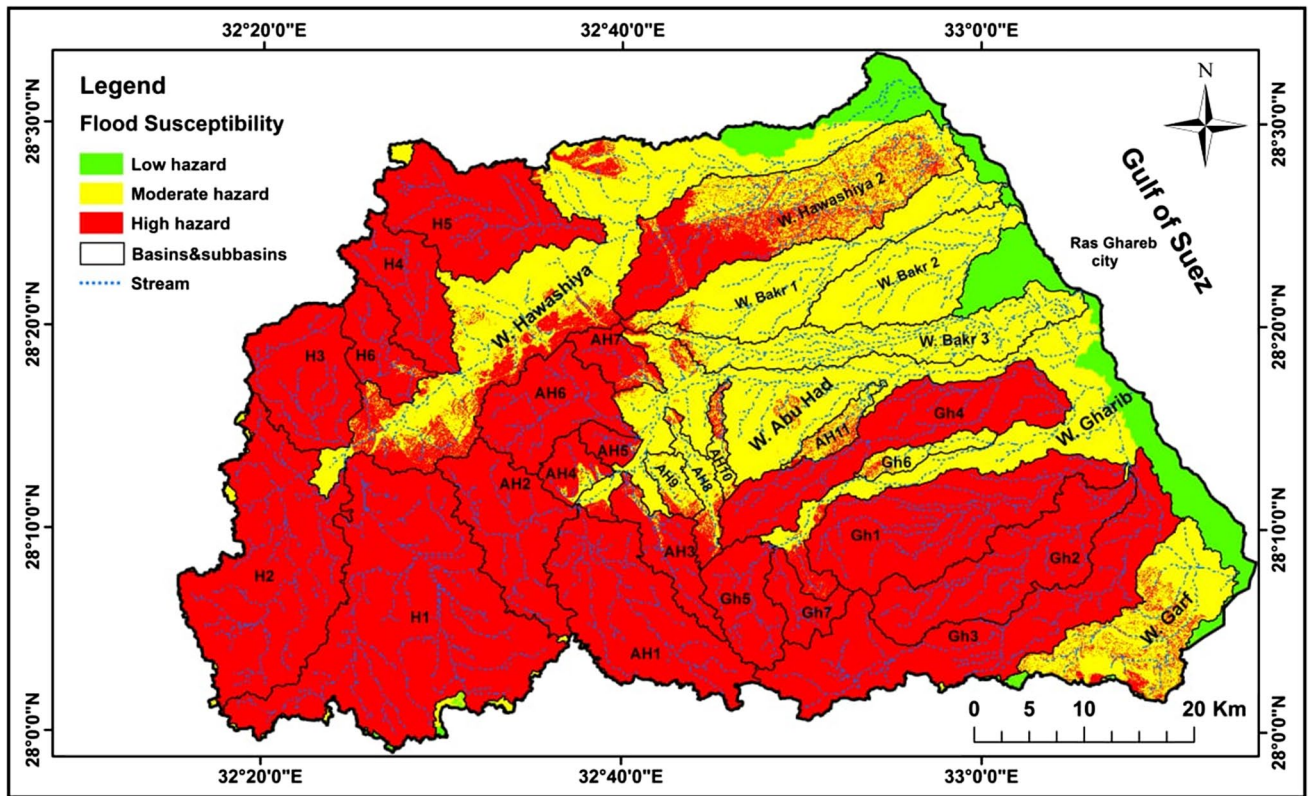| Class	Risk	Total score of all factors	Percent %
1	Low	<7	5
2	**Medium**	**7–13**	**33**
3	High	>13	62

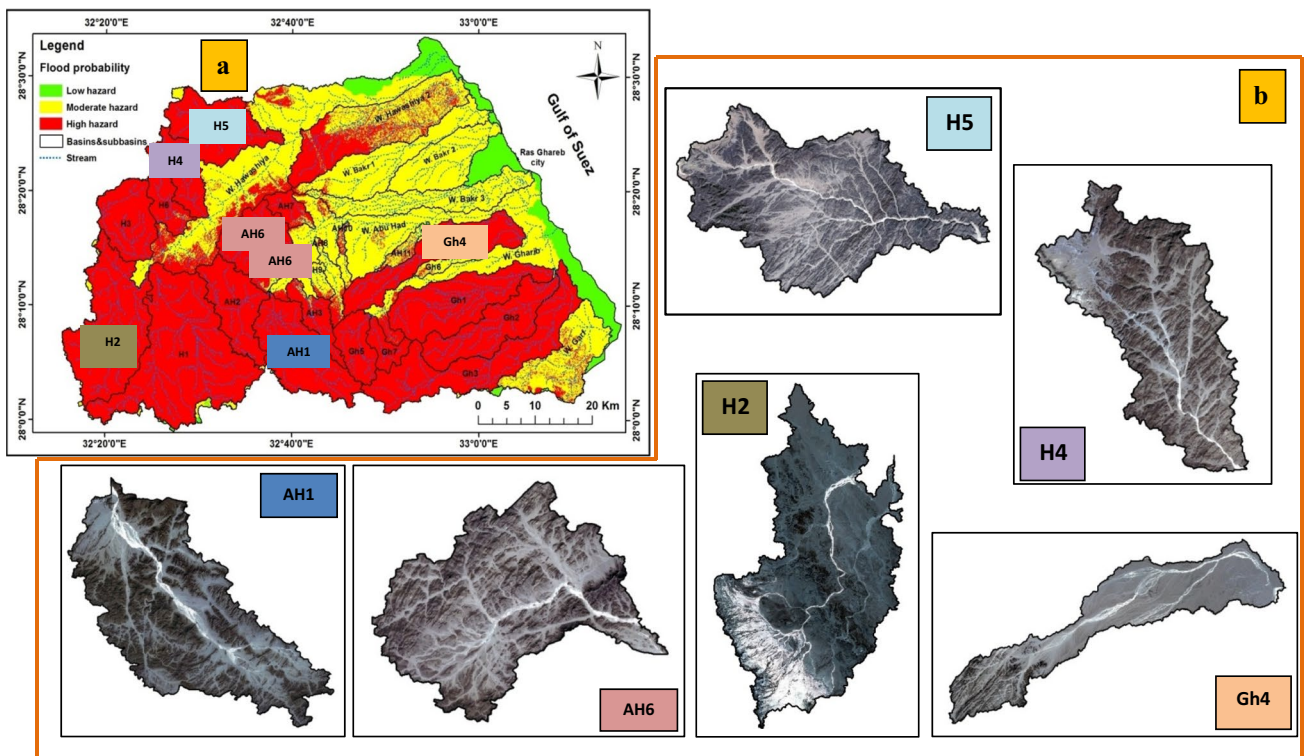**Fig. 17** Spatial distribution of flash flood susceptibility map of RG basins and related sub-basins

Fig. 18 Matching between flash flood hazard map (a) and some sub-basins extracted from Landsat image after occurrence flash flood

Fig. 19 Some pictures taken by residents for the RG flash flood of October 2016. (**a**, **b**) water in the streets up to 50 cm height, (**c**, **d**) photograph from an airplane showing the inundation problem for a large portion of the RG City, (**e**) a flash flood destroyed the main highway in the area and (**f**) photos from an airplane shows runoff water in desert areas
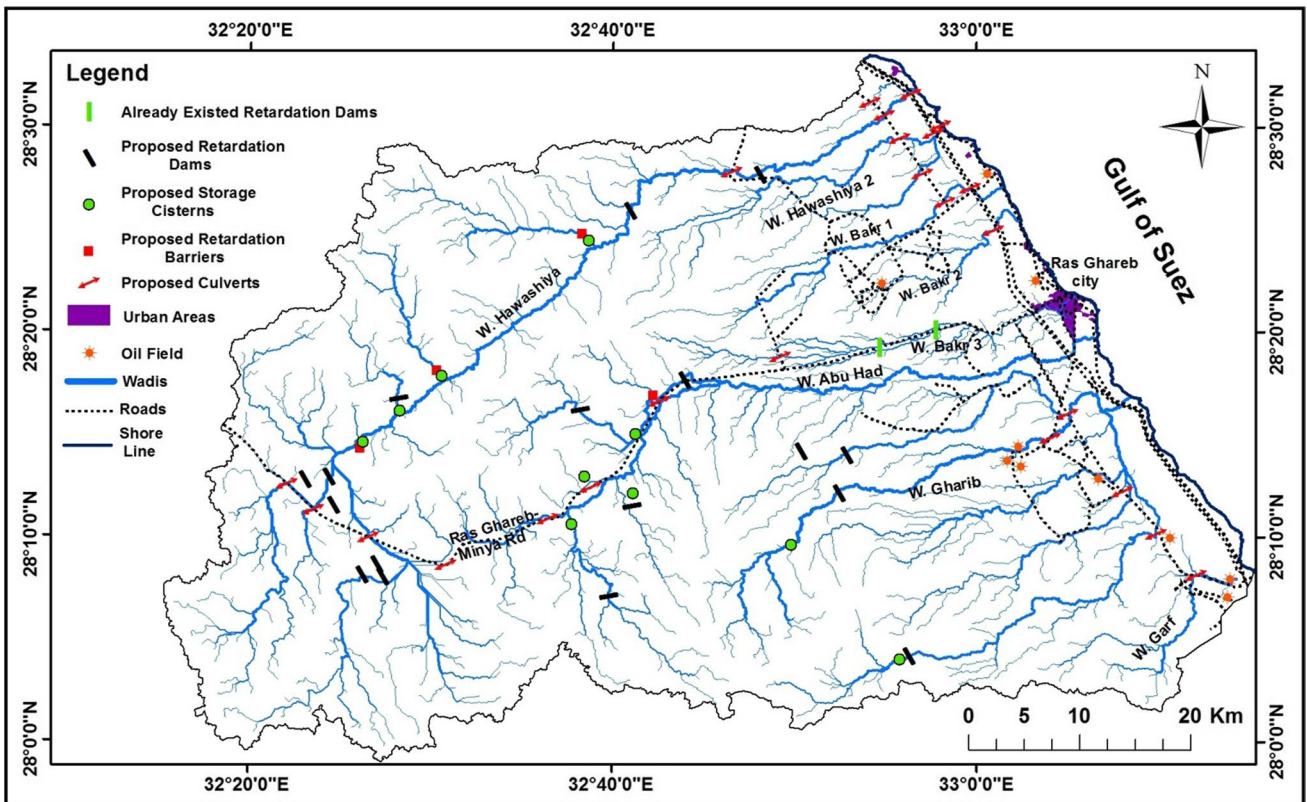
Fig. 20 Proposed locations of different mitigation measures for flash flood at RG area

high potential risk basins are concentrated in W. Hawashiya, especially at number H1, H2, and H5 sub-basins. Also, high risk occurs in W. Gharib, W, Hawashiya2, and W. Abu Had basins and Gh1, Gh2, Gh3, Gh4, AH1, and AH2 sub-basins. The three sub-basins are considered to have moderate risk, these sub-basins are H3, H4, and AH6; on other hand, there are sixteen basins and sub-basins that have a low risk. The topographic parameters potentiality mapping of the study area shows revealed the south and central parts of the RG area have high flood potentiality due to high slope gradients; however, most of the eastern areas have low flood potentiality due to gentle slopes. In addition, the south and western parts of the RG area have high flood potentiality due to high elevation gradients; however, most of the eastern areas have low flood potentiality due to gentle elevation. From point of the lithology and structural potentiality mapping, the study area could be divided into three classes of lithological hazard susceptibility in which the zones close to Precambrian rocks are the most vulnerable to flash flooding. Moreover, the eastern and western sections of the RG region have high flood potential; however, due to high-density fracture, most central areas have low flood potential. Moreover, the obtained rainfall hazard risk map of RG basins shows that the high-potential risk basins are concentrated in W. Hawashiya, W. Abu Had, and W. Gharib. One basin is considered to have moderate risk; this basin is W. Hawashiya 2. Three categories of flood hazard susceptibility that may be relevant to the RG area are depicted in the final risk map. The resulting final integrated flood hazard risk map indicates that 62% of the basins and sub-basins in the RG region have a high risk of flooding. Most of these sub-basins discharge into higher-order basins including the W. Hawashiya, W. Abu Had, and W. Gharib. A medium risk of flooding exists in 33% of basins and sub-basins of the RG area. The remaining basins and sub-basins, approximately 5%, are at low risk of flooding. The majority of the high-potential risk basins are centralized in W. Hawashiya, W. Abu Had, and W. Gharib. Furthermore, ten basins and sub-basins were designated as having a moderate flood risk. The findings substantially supported the model's validity as it was discovered that most integrated flash flood risk maps are consistent with Landsat imagery during the October 2016 flash flood incident in the RG region. Last but not least, the current study is able to use GIS and spatial multi-criteria analyses as efficient techniques to implement flash flood management systems and provide recommendations to decision-makers to conserve, mitigate, or at the very least lessen the devastating effects of floods in the studied areas.

References

Abrahams A (1984) Channel networks: a geomorphological perspective. Water Resour Res 20:161–168

Abuzied SM, Yuan M, Ibrahim SK, Kaiser MF, Saleem TA (2016) Geospatial risk assessment of flash floods in Nuweiba area, Egypt. J Arid Environ 133:54–72. https://doi.org/10.1016/j.jaridenv.2016.06.004

Aggour TA, Gomaa MA (2008) Hydrogeological and hydrogeochemical studies in Wadi Baba and Sidri, southwestern part of Sinai. Egypt Annals Geol Surv Egypt 497–528

Aglan OShA (1995) Geology of groundwater supplies in the area between Wadi Gharandal and Wadi Sidri, southwestern Sinai. Msc. Thesis, Geol. Dept., Fac. Sci., Ain Shams Univ. p 202

Arnous MO (2011) Integrated remote sensing and GIS techniques for landslide hazard zonation: a case study Wadi Watier area, South Sinai, Egypt. J Coast Conserv 15(4):477–497. https://doi.org/10.1007/s11852-010-0137-9

Arnous MO (2016) Groundwater potentiality mapping of hard-rock terrain in arid regions using geospatial modelling: example from Wadi Feiran basin, South Sinai, Egypt. Hydrogeol J 24(6):1375–1392. https://doi.org/10.1007/s10040-016-1417-8

Arnous MO, Green DR (2011) GIS and remote sensing as tools for conducting geo-hazards risk assessment along Gulf of Aqaba coastal zone, Egypt. J Coast Conserv 15(4):457–475. https://doi.org/10.1007/s11852-010-0136-x

Arnous MO, Omar AE (2018) Hydrometeorological hazards assessment of some basins in Southwestern Sinai area, Egypt. J Coast Conserv. https://doi.org/10.1007/s11852-018-0604-2

Arnous MO, Aboulela HA, Green DR (2011) Geo-environmental hazards assessment of the north western Gulf of Suez, Egypt. J Coast Conserv 15(1):37–50. https://doi.org/10.1007/s11852-010-0118-z

Arnous MO, El-Rayes AE, Geriesh MH, Ghodeif KO, Al-Oshari F (2020) Groundwater potentiality mapping of tertiary volcanic aquifer in IBB basin, Yemen by using remote sensing and GIS tools. J Coast Conserv 24:27. https://doi.org/10.1007/s11852-020-00744-w

Arnous MO, Mansour BM (2022): Utilizing multi-temporal thermal data to assess environmental land degradation impacts: example from Suez Canal Region, Egypt. Environ Sci Pollut Res. https://doi.org/10.1007/s11356-022-22237-z

Bajabaa S, Masoud M, Al-Amri N (2014) Flash flood hazard mapping based on quantitative hydrology, geomorphology and GIS techniques (case study of Wadi Al Lith, Saudi Arabia). Arab J Geosci 7:2469–2481. https://doi.org/10.1007/s12517-013-0941-2

Ball J (1916) The geography and geology of west central Sinai. Egypt. Surv. Dept, Cairo, p 219

Ball J (1937) The water supply of Mersa-Matruoh. Egypt. Survey and Mine Dept., Paper. No.42, Cairo, 18p

Bapalu VG, Sinha R (2005) GIS in flood hazard mapping: a case study of Kosi River Basin, India; Natural Hazard Management, ESRI. www.gisdevelopment.net

Bathrellos GD, Skilodimou HD, Soukis K, Koskeridou E (2018) Temporal and spatial analysis of flood occurrences in drainage basin of Pinios River (Thessaly, central Greece). Land 7(3):106

CEOS (2003) The use of earth observing satellites for hazard support: assessments and scenarios, final report of the CEOS Disaster Management Support Group (DMSG). Helen M. Wood, Chair. National Oceanic and Atmospheric Administration (NOAA) United States Department of Commerce

Chorely R, Donald M, Pogorzelsk H (1957) A new standard for estimating drainage basin shape. Am J Sci 255:138–141. https://doi.org/10.2475/ajs.255.2.138

Dawod GM, Mirza MN, Al-Ghamdi KA (2012) GIS-based estimation of flood hazard impacts on road network in Makkah city, Saudi Arabia. Environ Earth Sci 67(8):2205–2215

Dhiman R, VishnuRadhan R, Eldho TI, Inamdar A (2019) Flood risk and adaptation in Indian coastal cities: Recent scenarios. Appl Water Sci 9(1):5

Dube K, Nhamo G, Chikodzi D (2022) Flooding trends and their impacts on coastal communities of Western Cape Province, South Africa. GeoJournal 87(Suppl 4):S453–S468

Egyptian Geological Survey and Mining Authority "EGSMA " (1994) Floods of 1994, part 2, Red Sea Governorate. Cairo, 83 p. (In Arabic)

Egyptian Meteorological Authority (2006) Climatic atlas of Egypt. Ministry of Transportation and Communications, Cairo

El Nahry AH, Saleh AM (2005) Using remote sensing and GIS techniques for identifying influence of seasonal flashfloods on El-Qaa plain, Egypt. Proc. SPIE 5976, Remote Sensing for Agriculture, Ecosystems, and Hydrology VII, 597–604. https://doi.org/10.1117/12.621051

El Shamy IZ (1983) On the hydrogeology of west Central Sinai. Egypt Jgeol 27(1–2):93–105

EL-Rayes AE, Arnous MO, Aboulela HA (2015) Hydrogeochemical and seismological exploration for geothermal resources in South Sinai, Egypt utilizing GIS and remote sensing. Arab J Geosci 8(8):5631–5647. https://doi.org/10.1007/s12517-014-1667-5

El-Rayes AE, Arnous MO (2015) A novel approach in hydrogeochemical exploration for uranium mineralization: example from west central Sinai, Egypt. Acta Geol Sin (Engl Ed) 89(6):1895–11913. https://doi.org/10.1111/1755-6724.12606

El-Rayes AE, Arnous MO, Aziz AM (2017) Morphotectonic controls of groundwater flow regime and relating environmental impacts in Northwest Sinai, Egypt. Arab J Geosci 10:401. https://doi.org/10.1007/s12517-017-3188-5

EL-Rayes AE, Geriesh MH, Omran AF (2009) Flood control and water management in arid environment case study on Wadi Hagul, Gulf of Suez Region, Egypt. International Conf. on water conservation in arid regions, King Abdul Aziz Univ., Jedda, KSA, pp 1:28

Faniran A (1968) The index of drainage intensity- A provisional new drainage factor. Aus J Sci 31:328–330

Fernandez D, Lutz M (2010) Urban flood hazard zoning in Tucumán Province, Argentina, using GIS and multicriteria decision analysis. Eng Geol 111(1–4):90–99

Gardiner V (1990) Drainage basin morphometry. In: Goudie A (ed) Geomorphological techniques. Unwin Hyman, London, pp 71–81

Hadley R, Schumn S (1961) Sediment sources and drainage basin characterisics in upper Cheyenne River basin. US Geological Survey Water-Supply Paper 153-B, Washington DC, 198

Hallegatte S, Green C, Nicholls RJ, Corfee-Morlot J (2013) Future flood losses in major coastal cities. Nat Clim Chang 3(9):802–806

Hammad FA (1980) Geomorphological and hydrological aspects of Sinai Peninsula. A.R.E. Geol Surv Egypt 10:807–817

Hammad FA, Misak RF (1985) Quantitative geomorphology and groundwater possibilities in the vicinities of Wadi Nasib, Abu Zeneima, Sinai, Egypt. Desert Institute. Bull ARE 35(2):331–351

Horton RE (1932) Drainage basin characteristics: Trans Amer Geophys Union, 13. pp. 350–361

Horton RE (1945) Erosional development of streams and their drainage basins, Hydrophysical approach to Quantitative Morphology. Geol Soc Am Bull 56:275–370

Ivanova E, Nedkov R, Ivanova I, Radeva K (2012) Morpho-hydrographic analysis of black sea catchment area in Bulgaria. Procedia Environ Sci 14:143–153. https://doi.org/10.1016/j.proenv.2012.03.014

Komuscu AU, Erkan A, Celik S (1998) Analysis of meteorological and terrain features leading to the Izmir flash flood, 3–4 November 1995. Nat Hazards 18:1–25

Krishnamurthy J, Srinivas G, Jayaraman V, Candrasekhar M (1996) Influence of rock types and structures in the development of drainage networks in typical hardrock terrain. ITC J 3:252–259

Kumar R, Kumar S, Lohani AK, Nema RK, Singh RD (2000) Evaluation of geomorphological characteristics of a catchment using GIS. GIS India 9(3):13–17

Maidment DR (2002) Arc-Hydro GIS for water resources. ESRI Press, California

Martz LW, Garbrechet J (1992) Numerical definition of drainage network and sub catchment areas from digital elevation models. Comput Geosci 18(6):747–761

Miller VC (1953) A quantitative geomorphic study of drainage basin characterize in the Clinch Mountain area, Virginia and Tennessee. Columbia Univ Dept Geology Tech Report (3): p. 30

Mondal T, Gupta S (2015) Evaluation of morphometric parameters of drainage networks derived from topographic map and digital elevation model using remote sensing and GIS. Int J Geomat Geosci 5(4):655–664

Moubarak AH, Arnous MO, El-Rayes AE (2021) Integrated geoenvironmental and geotechnical risk assessment of East Port Said Region, Egypt for regional development. Geotech Geol Eng 39(2):1497–1520. https://doi.org/10.1007/s10706-020-01571-4

Nageswararao K, Swarna LP, Arun KP, Hari KM (2010) Morphometric analysis of Gostani River basin in Andhra Pradesh state, India using spatial information technology. Int J Geom Geosci 1(2):79–187

NHI "National Highway Institute" (2002) Highway hydrology. Hydraulic design series number 2 (2nd ed.), Publication No. FHWA-NHI-02–001, USA, 426 p

Omran A, Fahmida K, Schröder D, Arnous MO, El-Rayes AE, Hochschild V (2021) GIS-based rockfall hazard zones modeling along the coastal Gulf of Aqaba Region, Egypt. Earth Sci Inform 14(2):691–709. https://doi.org/10.1007/s12145-021-00580-y

Omran A, Schroder D, El-Rayes A, Geriesh M (2011) Flood hazard assessment in Wadi Dahab, Egypt based on basin morphometry using GIS techniques. In: Car A, Griesebner G, Strobl J (Eds): Geospatial crossroads @ GI_Forum '11. © Herbert Wichmann Verlag, VDE VERLAG GMBH, Berlin/Offenbach ISBN 978–3–87907–509–6

Papp F (2002) Extremes of extreme floods. In: A Snorasson, HP Finnsdottir, Moss M (Eds.) The extremes of the extremes: extraordinary

floods. IAHS Publication 271, Inter. Assoc. of Hydrologic Sciences, Davis, pp 373–378

Patton PC (1988) Drainage basin morphometry and floods. In: Baker VR et al (eds) Flood geomorphology. Wiley, New York, pp 51–65

Pradhan B (2010) Remote sensing and GIS-based landslide hazard analysis and cross-validation using multivariate logistic regression model on three test areas in Malaysia. Adv Space Res 45(10):1244–1256

Rai PK, Mohan K, Mishra S, Ahmed A, Mishra VN (2014) A GIS-based approach in drainage morphometric analysis of Kanhar River basin, India. Appl Water Sci 7:217–232. https://doi.org/10.1007/s13201-014-0238-y

Saad KF, El Shamy IZ, Sweidan AS (1980) Quantitative analysis of geomorphology and hydrology of Sinai Peninsula, 5th Africa Conference, A.R.E

Saleh A (1989) Flash floods in deserts. A geomorphic study of desert Wadis. Institute of Arab Res, Spec Stud Ser 51:1–93

Sameena M, Krishnamurthy J, Jayaraman V, Ranganna G (2009) Evaluation of drainage networks developed in hard rock terrain. Geocarto Int 24(5):1–24

Schumn SA (1956) Evaluation of drainage systems and slopes in the badlands at perth Amboy, New Jersy. Bull Geol Soc 67. pp 597–646

Shata AA (1955) Some remarks on the distribution of the carboniferous formations in Egypt. Bull Inst Des Egypt 5:241–247

Smith K (2013) Environmental hazards: assessing risk and reducing disaster. 6th edn, Routledge. https://doi.org/10.4324/9780203805305

Stern RJ, Hedge CE (1985) Geochronologic and isotopic constraints on late Precambrian crustal evolution in the Eastern Desert of Egypt. Am J Sci 285:97–127

Strahler AN (1952) Dynamic basis of geomorphology. Geol Soc Am Bull 63:923–938. https://doi.org/10.1130/0016-7606

Strahler AN (1957) Quantitative analysis of watershed geomorphology. Trans Am Geophys Union 138:913–920

Strahler AN (1964) Quantitative geomorphology of drainage basins is channel networks. In: Te Chow Vent (ed) Hand book of applied hydrology. McGraw Hill Book Company, New York, pp 39–79

Thorne CR (2002) Geomorphic analysis of large alluvial rivers. Geomorph 44(3–4):203–219. https://doi.org/10.1016/S0169-555X(01)00175-1

Wang Y, Zhang W, Liu X (2010) Hydrological watersheds model researching based on digital elevation model. 2010 18th International Conference on Geoinformatics, 18–20 June 2010, Beijing, pp 1–5, IEEE. https://doi.org/10.1109/GEOINFORMATICS.2010.5567929l

Xiao L, Liu H, Zhao X (2010) Impact of digital elevation model resolution on stream network parameters. Environmental Science and Information Application Technology (ESIAT), 2010 International Conference on (vol 3). https://doi.org/10.1109/ESIAT.2010.5568306

Youssef AM, Pradhan B, Hassan AM (2011) Flash flood risk estimation along the St. Katherine road, southern Sinai, Egypt using GIS based morphometry and satellite imagery. Environ Earth Sci 62(3):611–623

Youssef AM, Hegab MA (2005) Using geographic information systems and statistics for developing a database management system of the flood hazard of Ras Gharib area, Eastern desert, Egypt. The fourth international conference on the geology of Africa (2):1–15

Zerger A, Smith DI (2003) Impediments to using GIS for real-time disaster decision support. Comput Environ Urban Syst 27:123–141

Zhang XU, Zhou T, Zheng J (2009) DEM-based spatial discretization and parameter database design for distributed hydrological model. Proc. SPIE 7498, MIPPR 2009: Remote Sensing and GISData Processing and Other Applications, 749831 (October 30, 2009). https://doi.org/10.1117/12.832487